2014

Chemo-Mechanical Control of Neural Stem Cell Differentiation

Emily Rachel Geishecker
Lehigh University

Chemo-Mechanical Control of Neural Stem Cell Differentiation

By
Emily R. Geishecker

A Thesis
Presented to the Graduate and Research Committee
of Lehigh University
in Candidacy for the Degree of
Master of Science
in
Materials Science & Engineering

Lehigh University
January 2014

This thesis is accepted and approved in partial fulfillment of the requirements for the Master of Science.

_____

Date

_____

Thesis Advisor: Sabrina Jedlicka

_____

Chairperson of Department: Helen Chan

Acknowledgements

I would like to thank many people who have helped me through the completion of this thesis. The first is my advisor, Dr. Sabrina Jedlicka, for fostering my young research career in her biomaterials at Lehigh University. Additionally, the mentorship of Dr. Susan Perry was instrumental to me throughout my time at Lehigh, and her continued advice is invaluable. I have worked with many dedicated undergraduate researchers throughout the years; the best way to learn something is to teach it to someone else.

I am thankful for and would like to acknowledge many others who helped me along the way: my parents, for their continued support despite not knowing exactly what it is I do; my friends, for being there for me through my struggles and frustration ; and my colleagues, for their guidance and helpful suggestions. Finally, I would like to thank Chris Spagna for always cheering me up and standing by me through the good times and bad. I couldn't have done this without his support and encouragement.

The research was supported by NSF CBET #1014957. We also acknowledge the Lehigh University Faculty Innovation Grant (2009-2010 and 2011-2012). Additional thanks to Dr. Evan Snyder, of the Sanford-Burnham Medical Research Institute, for providing the C17.2 neural stem cells

Table of Contents

List of Figures

List of Tables

Abstract

Cellular processes such as adhesion, proliferation, and differentiation are controlled in part by cell interactions with the microenvironment. Cells can sense and respond to a variety of stimuli, including soluble and insoluble factors (such as proteins and small molecules) and externally applied mechanical stresses. Mechanical properties of the environment, such as substrate stiffness, have also been suggested to play an important role in cell processes. The roles of both biochemical and mechanical signaling in fate modification of stem cells have been explored independently. However, very few studies have been performed to study well-controlled chemo-mechanotransduction. The objective of this work is to design, synthesize, and characterize a chemo-mechanical substrate to encourage neuronal differentiation of C17.2 neural stem cells. In Chapter 2, Polyacrylamide (PA) gels of varying stiffnesses are functionalized with differing amounts of whole collagen to investigate the role of protein concentration in combination with substrate stiffness. As expected, neurons on the softest substrate were more in number and neuronal morphology than those on stiffer substrates. Neurons appeared locally aligned with an expansive network of neurites. Additional experiments would allow for statistical analysis to determine if and how collagen density impacts C17.2 differentiation in combination with substrate stiffness. Due to difficulties associated with whole protein approaches, a similar platform was developed using mixed adhesive peptides, derived from fibronectin and laminin, and is presented in Chapter 3. The matrix elasticity and peptide concentration can be individually modulated to systematically probe the effects of chemo-mechanical signaling on differentiation of C17.2 cells. Polyacrylamide gel stiffness was confirmed using rheological techniques and found to support values

published by Yeung et al. [1]. Cellular growth and differentiation were assessed by cell counts, immunocytochemistry (ICC), and neurite measurements. Data indicates that chemo-mechanical signaling is highly combinatorial in directing differentiation of C17.2s along a neuronal lineage *in vitro*.

Chapter 4 discusses the design, synthesis, and characterization of a novel nanomaterial platform to investigate ligand-receptor binding. PEGylated nanoparticles were successfully synthesized and found to be relatively homogenous in size and morphology, as observed by transmission electron microscopy. However, successful binding of RGD peptide to the nanoparticle was not confirmed.

Finally, a method for proteomic analysis of the C17.2 secretome is discussed in Chapter 5. Secreted proteins are of great importance as they can both influence cell behaviors as well as act as biomarkers of differentiation. Methods have been selected and optimized for protein extraction and two dimensional gel electrophoresis to be followed by mass spectrometry and protein identification. A temporal analysis of unique proteins expressed by C17.2s will result in a differentiation timeline. Deducing the dynamics of neuronal cell secretions will greatly contribute to the characterization of the C17.2 cell line and improve its relevance as a neural stem cell model.

Overall, results illustrate the importance of chemical and mechanical cues in manipulating neural stem cell fate. These material platforms in combination with the further characterization of the C17.2 neural stem cells could have a great impact in the fields of neuronal biology, translational therapeutics, and pharmaceutical research.

Chapter 1

Review of Current Literature

A cell's microenvironment has an enormous impact on the life and behavior of the cell. Processes such as adhesion, proliferation, and differentiation are controlled, in part, by interaction with the surroundings. Cells can sense and respond to a variety of stimuli, including soluble and insoluble factors such as proteins and small molecules, as well as externally applied mechanical stresses. Mechanical properties of the substrate, such as stiffness, have also been suggested to play a part in cell processes. Cells sense and respond to their environment via mechnaotransduction, a process in which the interaction with mechanical cues initiates intracellular signaling. The mechanical properties of the extracellular environment have been shown to greatly impact stem cell fate [2-4].

Biomimetic substrates designed to interface with stem cells is an important research interest in the realm of biomaterials and stem cell biology. Current methods to direct and maintain stem cells in culture are through the use of soluble proteins (growth factors) and adherent protein layers (ECM proteins). Despite its inherent benefits, traditional cell culture, solution phase approach is difficult to translate into therapeutic applications [5]. Additionally, i*n vitro*, adherent cells are typically cultured on rigid substrates that are orders of magnitude stiffer than their *in vivo* environments. It is generally hypothesized that cultured stem cells will function most optimally when *in vitro* conditions closely mirror the natural *in vivo* conditions. Engineered, biomimetic cell

culture substrates offer much promise as a valuable tool for stem cell culture with applications in implantable devices, drug delivery, and biosensors. One challenge in this area of research is deconvoluting the numerous factors, both biochemical and mechanical, associated with the *in vivo* environment. With further understanding of the impact of individual environmental factors, engineered culture surfaces would provide a level of control for researchers to manipulate stem cell fate to produce cells of a desired type, adding to the therapeutic potential of stem cell therapies.

The mechanical properties of the substrate (stiffness, roughness, topography, etc) are capable of influencing cell processes such as cell adhesion, migration, and differentiation in many cell types, including neural cells. Much of the work in the field of cell fate modification through mechanical properties of the extracellular environment focuses on substrate stiffness, or elasticity. Elasticity is defined as a material's ability to resist deformation [6]. Thus, stiffer substrates are less readily deformed than less stiff ones. The effect of surface elasticity seems to be cell-type specific, and seemingly related to the properties of the tissue of origin [1, 2]. Fibroblasts cultured on soft substrates have smaller spread area and shape factor than those on stiff substrates [7, 8], and even tune their internal stiffness to match that of their substrate [9]. In contrast, neurons have been seen to form three times as many branches on soft substrates as compared to stiffer surfaces [10].

Control and manipulation of cell fate has been an important tool for use in stem cell research and development of stem cell-based therapeutics. In addition to traditional chemical based methods, the Discher lab at the University of Pennsylvania showed that

stem cell fate can be influences by the elasticity of the matrix microenvironment [3]. While the importance of the mechanical properties of the ECM had been established in morphological, adhesion, and motility studies with fibroblasts and tumor cells [11, 12], this study was the first to differentiation stem cells solely through substrate elasticity. Mesenchymal stem cells (MSCs), adult multipotent stem cells from bone marrow, were cultured on polyacrylamide gel substrates of various stiffnesses. MSCs cultured on soft substrates mimicking the elasticity of brain tissue (<1kPa) showed a neuronal phenotype. Cells cultured on substrates of intermediate stiffness similar to striated muscle (10kPa) showed myoblast-like morphology, and those cultured on stiff gels similar to the elasticity of bone (100kPa) began to resemble osteoblasts. Immunocytochemical staining for neuronal, muscle, and bone markers, as well as PCR analysis, corroborated morphological observations. However, limited expression of markers of terminal differentiation was observed. The investigators concluded that matrix elasticity can initially direct MSCs to a particular lineage, but is insufficient for full differentiation [3]. This study provided a very powerful tool for investigating the control of stem cell differentiation through modulation of the culture environment.

In vitro investigations of the role of substrate stiffness on cell behavior are typically carried out on a select few material substrates. Polyacrylamide gels are one of the most commonly used substrata for mechanotransduction experiments due to their mechanical tunability and optical transparency. Polyacrylamide is an highly elastic uncharged hydrophilic polymer which stiffnesses depends of the density of crosslinks formed by N,N-methylene-bis-acrylamide monomer [1]. Materials across a broad

physiologically relevant stiffness range (0.01-100kPa) can be formed while maintaining a constant network topography and surface chemistry. Neither cells nor their secreted proteins bind to polyacrylamide, so cell adhesion can be controlled independently of stiffness through covalent crosslinking of collagen [1]. Other polymer systems, such as polyethylene glycol [13], alginate [14], agarose, [15] and polydimethyl siloxane (PDMS) [16] have also been used in 2D and 3D configurations. Although the mechanical properties of PDMS are easily tunable across physiologically relevant moduli, the surface chemsitry, and thus cell response, is also affected [17].

The method through which cells sense their mechanical environment is not trivial, and it is likely that there are multiples types of mechanosensors including stretch-sensitive ion channels [18], mechanically actuated protein unfolding [19], and changes in protein kinetics, i.e. actin stabilization [20]. Recent studies have shown that cell adhesion cites not only sense the chemical properties of the cell's microenvironment (e.g. ECM ligands, adhesion molecules), but are also capable of sensing mechanical cues such as applied mechanical stresses and deformation [11, 21-25]. Additionally, it can be difficult to experimentally distinguish between a mechanosensor from a chemical or mechanical pathway since physical linkages necessary in the mechanosensor pathway may be disrupted by experimental treatments. For example, it is difficult to distinguish between the possible mechanosensitivity of integrins themselves and the necessity of integrin cell anchoring for mechanotransduction through other pathways [26].

In a study performed by Pelham and Wang in 1997, the mechanism of cellular interaction with the surrounding environment was investigated [7]. Like other studies, the

effect of substrate stiffness of cell spreading and mobility was explored. Beyond this, the morphology and dynamics of focal adhesions of normal rat kidney epithelial and 3T3 fibroblastic cells were observed. Focal adhesions are micron-scale structures that provide a structural link between the actin cytoskeleton and the ECM through integrins forming a multicomponent signaling complex upon activation [27]. They conjectured that cells sense their mechanical environment through the points of attachment, that focal adhesion complexes were involved in both outside-in and inside-out signaling. Visualization of fluorescently labeled vinculin, a focal adhesion complex protein, indicated that stable focal adhesions were formed by cells cultured on stiff substrates, while those cultured on soft substrates had irregularly shaped and highly dynamic focal adhesions. Additionally, the extent of tyrosine phosphorylation, an event involved in focal adhesion signaling [28-30] was found to correlate with focal adhesion data, further implicating this pathway in mechanotransduction [7].

In a 2005 study by Yeung *et al*., the investigators examined the effect of substrate stiffness or an extended range of cell types, including NIH3T3 fibroblasts, bovine aorta endothelial cells, and human neutrophils [1]. They observed that mechanical effects of surface elasticity depend on both cell type and adhesion receptor binding. Fibroblasts and endothelial cells were both shown to develop more actin stress fibers and spread more fully on stiffer substrates, while neutrophils appeared insensitive to variation in surface stiffness. Integrin subunit α5 was unregulated in fibroblasts cultured on stiffer substrates, interpreted as an increase in adhesivity on stiffer materials. Exogenous expression of α5 was insufficient to promote cell adhesion to softer gels. Both with and without engineered

α5 expression, fibroblasts exhibit a more spread morphology on stiff gels, than the compact, circular morphology seen when cultured on softer substrates [1].

While the Yeung et al. study expanded the range of cell types studied on mechanically varied surfaces, until very recently little attention had been paid to neural cells. Historically, reports have been mixes as to whether neural stem cells are sensitive to mechanical stimuli. *In vivo,* neural cells do not experience stresses of the same magnitudes as other cell types, such as osteoblasts or myocytes [31, 32]. However, the ability of neurons to respond to physical stimuli is essential in outgrowth during neural development and regeneration. During development, neural cells migrate and align in a spatiotemporally specific manner to form a functional nervous system [33, 34]. Environmental guidance cues present during growth cone development and nerve regeneration can greatly influence the growth and behavior of neural cells [35-40]. These cues, experienced by cells *in vivo,* can provide us with great insight to the factors that affect differentiating cells in the neural environment.

In a 2011 study, differentiated neuroblasts were seeded into poly(dimethylsiloxane) channels with localized surfaces with elastic moduli of 800kPa and 200kPa next to one another. They found that, depending on the position of the soma, cell processes responded to the interface of materials of varying stiffnesses by turning back, aligning along, or crossing over the boundary [41]. Although the moduli examined in this study are not of physiological relevance, it shows that cells are able to sense and respond to the difference in substrate stiffness.

In recent years, several studies have been performed to investigate the effect of substrate stiffness on neural stem cell differentiation in a similar manner to the Engler 2006 work with hMSCs. Neural stem cells can give rise to all three neural cell types – neurons, astrocytes, and oligodendrocytes. This lineage commitment has been seen to be mechanosensitive; NSCs generate more neurons when cultured on soft substrates (<1 kPa) and more astrocytes on hard substrates [42, 43]. These studies considered only initial neuronal lineage commitment to any type of neuron ("pan-neuronal") rather than mature neuron subtype or physiological function. In a 2013 study, it was observed that ECM stiffness did not impact the expression of NeuroD1, TrkA/B/C or the percentages of pan-neuronal, GABAergic, or glutamatergic neuronal subtypes in differentiated primary rat hippocampal NSCs [44]. NeuroD1 is a transcription factor whose expression peaks at the time of neuronal lineage committment and tyrosine kinase neurotrophin receptors TrkA/B/C, responsive to neurotrophic factors, are expressed within the first day of neuronal differentiation and maintain expression throughout neuronal subtype maturation [45]. Based on analysis of both protein and gene expression following NSC differentiation, the investigators concluded that neuronal subtype specification is not affected by substrate stiffness [44].

The work presented in this study is an expansion on research completed by Colleen Curley of the Jedlicka lab. Colleen investigated the effect of substrate stiffness on specific aspects of C17.2 neural stem cell differentiation, including neurite growth, synapse formation, and mode of division. Colleen showed that, like with other NSCs, soft gel substrates provide an optimal culture surface for differentiation of C17.2s into

neurons. These substrates supported populations with the longest neurite extensions and expression of pre-synaptic and post-synaptic proteins. In Colleen's work, collagen was used to promote cell adhesion at a constant concentration to allow for examination of the effect of substrate stiffness alone. By isolating mechanical stiffness, she was able to characterize the effect of this factor alone on the differentiation of C17.2 neural stem cells [46]. This understanding serves as the foundation for the study presented here, which combines the effects of substrate stiffness with changes in collagen concentration and ECM peptide functionalization.

The ECM is an intricate network of fibrous proteins and polysaccharides that provides essential physical scaffolding as well as initiating crucial biochemical and biomechanical cues [47]. Although the ECM throughout the body is fundamentally composed of water, proteins, and polysaccharides, each tissue has a unique composition creating a unique cellular microenvironment. Cell recognition of and adhesion to the ECM is mediated through integrins. As discussed earlier, integrins are transmembrane receptors that connect the cytoskeleton to the extracellular space. These receptors are extremely important in development, due to the adhesive function and capacity to modulate signal transduction pathways affecting gene expression [48, 49]. Each ECM molecule possesses multiple integrin ligands [50-53]. Integrins recognize several amino acid sequences within ECM proteins, one of the best known being RGD found in fibronectin and several other ECM proteins [54, 55]. Integrin-ligand binding initiates the formation of focal adhesion complexes, comprised of integrin clusters and additional signaling and structural proteins [56, 57], which can further influence cell behaviors such

as migration, proliferation, and differentiation. The design of a material platform to provide expound extracellular cues provides an additional handle to influence cellular fate.

While traditionally used to promote cell adhesion, ECM proteins and peptides can also be selected to control cell fate. Differentiation of endothelial cells has been seen to be markedly accelerated by culture on a substrate composed of basement membrane proteins, of which laminin is a primary constituent [58]. ECM also plays a vital role in the developing neural environment: distribution of ECM molecules defines the migratory pathways in the neural crest [59-61], and integrins have been seen to be upregulated on the surface of migrating crest cells [62, 63]. Neurons from a variety of sources and species extend neurites on substrates coated with purified laminin [64-77]. In addition to presence of ECM proteins, optimal concentration and gradients of these molecules is critical. Collagen concentration has been seen to effect chondrogenic differentiation of hMSCs [78, 79]. When embryonic stem cells were cultured in networks of various compositions of collagen, fibronectin, and laminin, differentiation was limited on high collagen concentration materials due to inhibition of apoptosis. Fibronectin stimulates endothelial differentiation and vascularization of embryonic stem cells, while laminin encourages differentiation of ES cells into beating cardiomyocytes [80]. When sensory neurons are cultured on substrates with varying concentrations of bound laminin, the amount of receptor ($\alpha_6\beta_1$ integrin) is post-translationally regulated by altering the integrin reuptake rate. Low ligand availability increases the amount receptors on the surface of the sensory neurons which leads to increased adhesion and neurite outgrowth,

while decreasing integrin RNA and total integrin protein expression [81]. The study presented here explores the effect of different collagen concentrations, in combination with varied polyacrylamide substrate stiffness, on the neuronal differentiation of C17.2 NSCs.

Many ECM substrate coatings, such as the collagen used in this study, are animal derived whole proteins which are difficult to control, interpret, and reproduce. Additionally, changes in the global conformation of the protein alter the presentation of integrin binding sites, altering efficiency of cell binding [82-84]. As a result, whole extracellular protein protocols can be difficult to reproduce and even more difficult to translate into *in vivo*. One challenge in using whole collagen with the polyacrylamide platform is that collagen (and other ECM protein) conformation is very likely linked to substrate mechanics and will likely change with substrate mechanical compliance. Therefore, an alternative approach was taken using synthetic mixed peptides, similar to those previously described [85-87]. Known cell binding sites from ECM proteins were synthesized using Fmoc solid state chemistry methods. The use of synthetic peptides allows for independent manipulation of ligand combinations and concentrations without the challenge of controlling conformation. The work presented here explored the use of peptide-functionalized polyacrylamide gels to study the individual contributions of biochemical and mechanical cues to neuronal differentiation. Substrates were functionalized with mixed adhesive peptides, derived from fibronectin and laminin, based on previous work by Jedlicka et al. [88].

In addition to chemical signaling of integrin-peptide binging, the actual binding interaction between receptor and ligand is capable of inducing downstream signaling events, though the mechanics of binding are involved in this signaling. By translating the 2D peptide-modified material system into a nanoparticle platform, it would be possible to investigate and quantify the effects of integrin-ligand binding, and potentially alter cell fate through nanoparticle-cell interaction [89-90]. The hypothesis driving this work is that biomechanical forces coupled with biochemical integrin-ligand interactions are capable of initiating downstream signaling processes, and thus affecting cell differentiation. In the study that will be presented in Chapter 3, peptide functionalized PEGylated silica nanoparticles are conjugated with peptide molecules that mimic the natural receptor ligand in order to provide selective targeting to integrin receptors of interest. Mechanical properties of the NPs can me modulated based on PEG length, allowing for a combined chemical and mechanical signaling in a single NP platform. This work aims to synthesize and characterize PEGylated SiO_2 NPs, with and without peptide modifications, for future use in force analysis of ligand-cell binding. Not only does the PEG contribute its mechanical properties, it also improves particle dispersion in water and media and reduces the rate of degradation [91].

C17.2 neural stem cells, a gift from Dr. Evan Snyder at the Burnham Institute, serve as the cell model for this work. These cells, originally isolated from external germinal layer of neonatal (P4) mouse cerebellum, are genetically engineered via retro-virus-mediated v-myc transfer to augment stem-like behavior [92]. These have been characterized extensively in implantation studies [37, 93, 94], and our group has been

working to characterize their behavior *in vitro*. Part of this characterization has been the analysis of the C17.2 secretome throughout the 21 day differentiation period. Unique proteins secreted at particular time points during differentiation hold promise for use as biomarkers. Similar characterizations have been performed for other differentiating cell types, such as myoblasts and enterocytes [95-97].

Secreted proteins from neural cells serve a crucial function in the nervous system. In the brain, secreted proteins can act as chemoattractants or chemorepellants, which play a large role in the regulation of neural progenitor cell migration [98]. These secreted proteins combine with the extracellular environment to affect the interaction between neural cells and their substrates, and eventually impacting differentiation [99-100]. A temporal analysis of the C17.2 secretome will result in a differentiation timeline. Deducing the dynamics of neuronal cell secretions will have a major impact on neuronal biology, translational therapeutics, and pharmaceutical research.

This research project aims to evaluate a wide range of the extracellular conditions, including substrate stiffness, collagen concentration, ECM peptides, and integrin-ligand binding forces, in order to identify the optimal in vitro environment for NSC differentiation– knowledge that has promising implications for tissue engineering.

:

Chapter 2

Chemo-Mechanical Control of C17.2 Neuronal Differentiation

Introduction

A cell's microenvironment is known to influence cellular processes such as adhesion, proliferation, and differentiation [101, 102]. *In vivo*, the intercellular space is filled with a unique assembly of extracellular matrix (ECM) proteins. Cells interact with ECM proteins through integrin receptors in the cell membrane and induce signaling cascades within the cell. The surrounding cues can cause the cell to divide, differentiate, migrate or even undergo apoptosis. Cues that influence cell fate include biochemical factors such as hormones and proteins. While activation of signal transduction pathways by interaction of integrins and bioactive peptides has been well studied, physical properties of the microenvironment also play a role in stem cell differentiation [11, 21]. Mechanical cues include surface topography, shape and stiffness. Matrix elasticity has been observed to direct stem cell lineage specification. Human mesenchymal stem cells have been reported to differentiate into various cell types including neurons, myoblasts, and osteoblasts, depending on the culture substrate stiffness [3]. Cells are capable of both applying force to the substrate as well as responding to matrix stiffness through cytoskeletal reorganization, migration, and differentiation [11]. Together, these cell-surface interactions are part of the mechanisms by which a cell converts mechanical stimuli to biochemical signals, or mechanotransduction.

While both biochemical and mechanical signaling have been explored independently, very few studies have been performed to study well-controlled chemo-mechanotransduction. With regards to proliferation and differentiation of stem cells for therapeutics, a chemo-mechanical approach may have profound effects on potential clinical translation. The objective of this work is to design, synthesize, and characterize a chemo-mechanical substrate to encourage neuronal differentiation C17.2s.

Neural stem cells (NSCs) are used as a model to study cell-ECM interactions associated with the developing neural environment, as well as providing insight in the development of scaffolds for neuronal regeneration. C17.2 neural stem cells serve as the cell model for this work. These cells, originally isolated from neonatal mouse cerebellum, are genetically engineered to augment stem-like behavior [92]. They have been characterized extensively in implantation studies [37, 93, 94], though their *in vitro* characterization is limited. NSCs can give rise to multiple cell types, including neuronal, astrocyte, and oligodendrocyte lineages, in response to distinct cues (Reynolds 1992). C17.2s differentiation through serum withdrawal produces a mixed population of cells depending on culture conditions. As seen in figure 2.1, we have seen them differentiate into neurons expressing β-tubulin III, glial-fibrillary acidic protein-positive astrocytes, and what we believe to be radial glia or basal progenitor cells. During neural development, extracellular cues can promote differentiation of NSCs into cells of mature phenotypes [103]. Cellular response to such stimuli has been well characterized [104-106]. Synthetic scaffolds have been developed to study the effect of immobilized ligands on NSC differentiation [107-110]. These surfaces containing ECM proteins and peptide

sequences have been observed to modulate cell fate and function. Identifying specific factors in the microenvironment, such as biochemical factors, as well as understanding the effect of matrix stiffness will provide new tools to promote stem cell differentiation into a particular lineage.

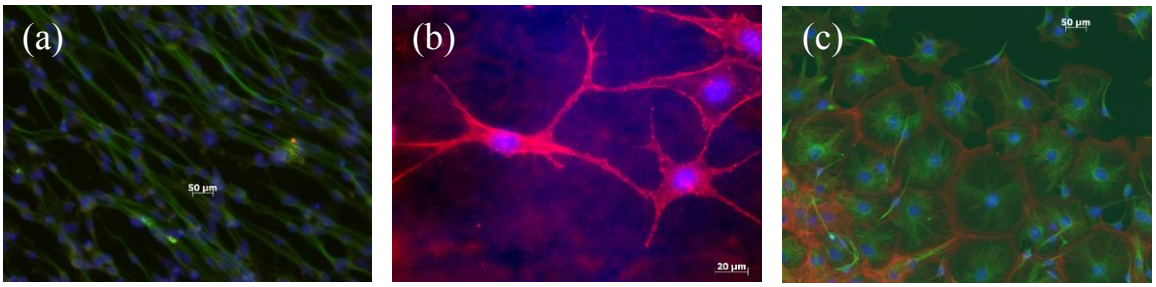

Figure 2.1. Differentiated C17.2 cells stained for (a) β-tubulin(III) (green), a neuronal marker, and nuclei (blue), (b) Glial Fibrillary Acidic Protein (red), an astrocytic marker, and nuclei (blue), and (c) Nestin (green), a neural stem cell intermediate filament protein, Actin (red), a cytoskeletal protein, and nuclei (blue).

In order to investigate the role of substrate stiffness, polyacrylamide (PA) gels are used as cell culture substrates, due to their biocompatibility, ease of sterilization, and tunability of modulus. The elastic modulus of the PA gels is easily controlled by adjusting the ratio of acrylamide and bis-acrylamide monomers used to form the material. The greater the percentage of bis-acrylamide, the greater the cross-linking between the molecules and the stiffer the substrate becomes.

Materials and Methods

Polyacrylamide Substrate Fabrication: Polyacrylamide (PA) gels of 100µm thickness were prepared according to the method of Yeung et al. with slight modification [1]. Briefly, glass coverslips (VWR) were flamed, coated with 0.1N NaOH, and air dried.

Coverslips were then coated with a thin layer of (3-aminopropyl) trimethoxysilane (Acros Organics) and dried for 15 minutes. Coverslips were then washed thoroughly with ddH_2O and subsequently incubated in 0.5% glutaraldehyde (Alfa Aesar) in 1X PBS for 30 minutes at room temperature. Coverslips were washed again in ddH_2O, dried, and used immediately or stored for up to several weeks in a dry place.

High, medium, and low stiffness gels were created by varying the ratio of acrylamide and bis-acrylamide monomer in the gel solution, according to Table III in Johnson et al. 2007. Precursor solutions were made from acrylamide (40% in ddH2O), N,N'-methylenebisacrylamide (2% in ddH2O), and HEPES (0.5M, pH 4.22). Gel components were combined and degassed for 30 minutes [111]. Following degassing, ammonium persulphate was added to a final concentration of 0.05% to initiate crosslinking. The acrylamide solution was then pipetted onto each amino-silanated coverslip (20 μL per 22mm square coverslip) and topped with a round Rain-X coated 18mm round coverslip (modified to prevent adherence to the gel). The gels were allowed to polymerize for 25-60 minutes, top cover glass was removed, and gels were used immediately or stored in HEPES (50mM, pH 8) for up to two weeks.

	Low	**Medium**	**High**
% Acrylamide/% Bis-acrylamide	3 / 0.04	3 / 0.1	10 / 0.5

Table 2.1. Ratio of Acrylamide to Bis-acrylamide for gel compositions used in this study [11].

In order to promote cell attachment, collagen was covalently conjugated to the polyacrylamide gel using the heterobifuctional crosslinker, N-Sulfosuccinimidyl-6-(4'-

azido-2'-nitrophenylamino) hexanoate (Sulfo-SANPAH, Thermo Scientific). Polyacrylamide gels were briefly dried to remove excess water before 100μL of the Sulfo-SANPAH solution (0.5 mg/mL in HEPES, pH 8.0) was pipetted onto the surface of each gel. The gels were then irradiated under UV at a distance of 6 inches for 15 minutes to initiate light-activated binding of the Sulfo-SANPAH to the polyacrylamide. The Sulfo-SANPAH solution was aspirated and samples were then washed thoroughly with 50mM HEPES (pH 8). A collagen solution of 0.1, 0.2, or 0.4 mg/mL was added to each sample (2 mLs/well). Samples were incubated for greater than 8 hours in the collagen solution and sterilized under UV prior to cell seeding.

Viscoelastic Characterization: The viscoelastic properties of polyacrylamide gels were quantified by measuring the dynamic shear moduli using an ARES rheometer (TA Instruments). Low- and medium-stiffness gels were assessed using the couette fixture. Samples were polymerized *in situ;* solution was pipetted into the fixture and covered with mineral oil. Time sweep readings were taken every 10 minutes over three hour polymerization period. The shear storage modulus G , corresponding to the stiffness of the gels, was determined from the shear stress in phase with an oscillatory (1 rad/s) shear strain of 50% maximal amplitude. Medium- and high-stiffness samples were polymerized between two 25-mm glass parallel plates that were previously activated in the same method as glass coverslips (described above) with a corresponding sample thickness of approximately 1 mm. Fixture was wrapped in parafilm during polymerization to reduce air exposure of the gel. Readings were taken one hour after gel-casting, to ensure near complete polymerization. Strain sweep readings were taken from

15 to 50% and 15 to 70% strain amplitude for the medium and high stiffness samples, respectively, with a frequency of 1 rad/s.

Cell Culture: C17.2 neural stem cells, obtained from Dr. Evan Snyder at the Burnham Institute, were maintained in high-glucose DMEM containing 10% FBS, 5% horse serum, and 2mM L-Glutamine. Cells were passaged at 80-90% confluency using cell stripper. All experiments were performed with cells at passage number 20 or below. Media was changed 3 times per week by removing half of the old culture media and replacing with fresh media. For the serum withdrawal procedure, cells were fed in a similar manner every 2 days, removing half of the media and replacing with serum-free culture media (DMEM high glucose with 1% L-Glutamine), essentially reducing the serum content by 50%. Cells were seeded onto the polyacrylamide gel substrates at a density of 10,000 cells/cm^2 and allowed to grow to about 80% confluency, at which point the serum withdrawal process began. Cells were cultured for 21 days (14 days below 1% serum) and then fixed with paraformaldehyde. Cells were imaged using phase contrast microscopy throughout the culture period to assess adherence to the PA substrates.

Immunocytochemistry: Following 21 days of serum withdrawal, cells were fixed with 4% paraformaldehyde in 1X PBS for 15 minutes. Samples were rinsed three times with PBS and permeablilized in 0.1% Triton X-100 in PBS for 15 minutes. Three additional rinses were performed, and cells were then blocked with 1% BSA in 0.01% Triton X-100 for 15 minutes. Samples were incubated in primary antibody solution (1:1000 anti-β-tubulin III-AF488 (Covance) and 1:100 anti-Nestin (DSHB) in 0.001%Triton X-100 + 0.1% BSA in PBS) at 37°C for 2 hours, and overnight at room temperature. Samples

were then rinsed with PBS and counterstained with Hoechst dye (0.002 mg/mL in ddH_2O, Invitrogen). Additional rinses were performed and samples were left in PBS for imaging.

Collagen Quantification: Quantification of collagen on the polyacrylamide gels was achieved by densiometric analysis of SDS-PAGE. Gels of each stiffness (high, medium, and low) were functionalized with collagen (0.1, 0.2, and 0.4 mg/mL) as described above. A curve was created with collagen standards ranging from 0.4-0.025 mg/mL in 50mM HEPES (pH 8) for a total well volume of 2 mL. Standard samples were air dried to remove all solvent. To release the collagen from the samples, collagen was digested with collagenase Type I (0.1 mg/mL in 10mM HEPES + 5mM $CaCl_2$, CalBiochem) for 2 hours at 37°C on a rocker, using the same volume for all samples. 5X sample buffer + EDTA (0.1μM final concentration) was added to terminate the digestion.

The digestion products were analyzed by using sodium dodecyl sulfate polyacrylamide gel electrophoresis (SDS-PAGE) on a 7% gel to resolve the TCA and collagenase bands and on a 10% gel to resolve the TCB fragments. Gels were run at 75mA for 6 hours and stained with Coomassie Brilliant Blue.

Results and Discussion

Viscoelastic Characterization: Dynamic Mechanical Analysis was performed on the high, medium, and low stiffness polyacrylamide gels to confirm elastic modulus values. High and medium stiffness samples were analyzed using a parallel plate geometry. To eliminate material slipping issues associated with other fixtures and geometries, glass

plates were activated in an identical manner to the coverslips, allowing for covalent attachment of the polyacrylamide to the fixtures. The gets were cast *in situ* and allowed to polymerize for one hour. A dynamic strain sweep was performed. If the modulus remains relatively constant across the strain sweep, it can be accepted as reliable. Figures 2.2 and 2.3 show the average strain sweep curve for 7 runs for the medium and high stiffness gels, respectively. These graphs, showing G', or elastic modulus, vs. strain amplitude, show that the values obtained are reasonable consistent over the strain amplitude range. The medium gel was found to be approximately 180Pa and the high stiffness gel around 15,000Pa.

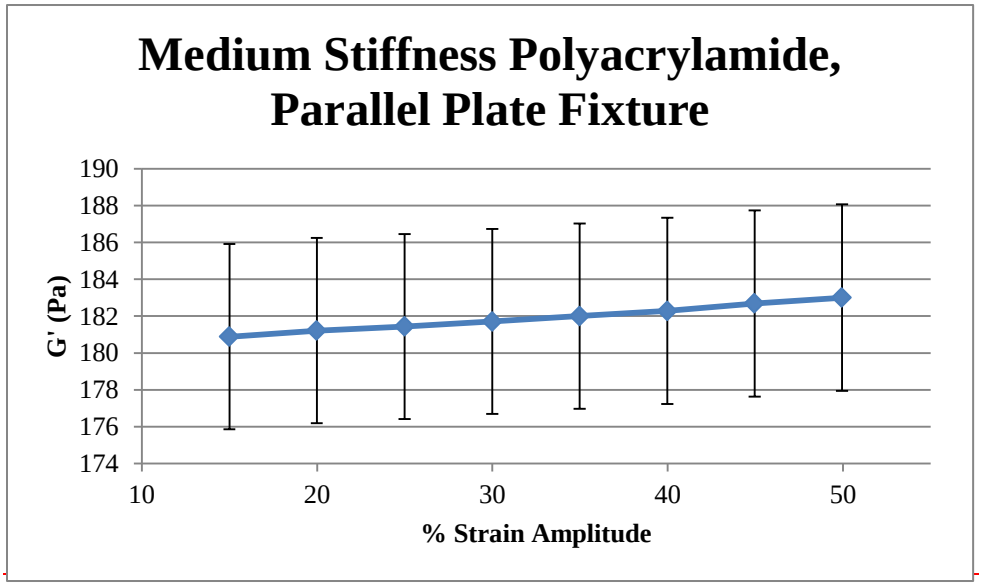

Figure 2.2. Modulus vs. % Strain Amplitude for medium stiffness polyacrylamide. Material was polymerized for one hour between activated glass parallel plates prior to data collection. Error bars represent standard error, n=7

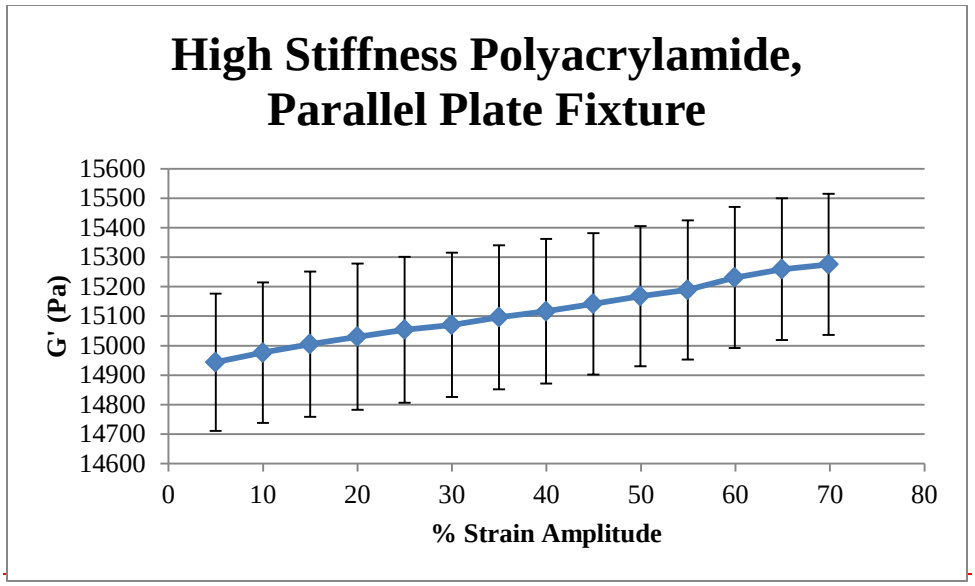

Figure 2.3. Modulus vs. % Strain Amplitude for high stiffness polyacrylamide. Material was polymerized for one hour between activated glass parallel plates prior to data collection. Error bars represent standard error, n=7

The low stiffness sample was not able to fully polymerize in this geometry, thus a different fixture was used. Instead of parallel plates, a cup and bob, also referred to as a couette, fixture was used. The fixture was loaded with polyacrylamide solution, and a time sweep reading was taken across the course of polymerization (3 hours), shown in Figures 2.4 and 2.5. This provides a clear view of the polymerization timeline. For consistency, readings were also taken of the medium stiffness gel. Unfortunately, the modulus of the high stiffness gel was too high for use with this fixture and overloaded the instrument. The low stiffness sample fully polymerized after 100 minutes and showed a modulus of approximately 150Pa. The medium stiffness gel polymerized slightly quicker, as expected, in 50 minutes. Its elastic modulus was found to be 560Pa.

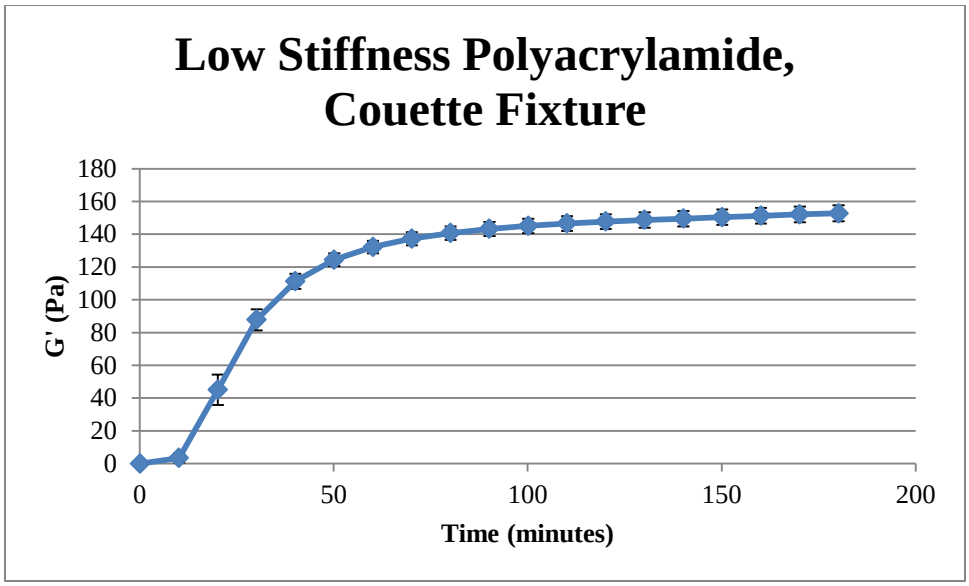

Figure 2.4 Modulus vs. time for low stiffness polyacrylamide. Material was loaded into coquette fixture and data was collected throughout polymerization. Error bars represent standard error, n=5

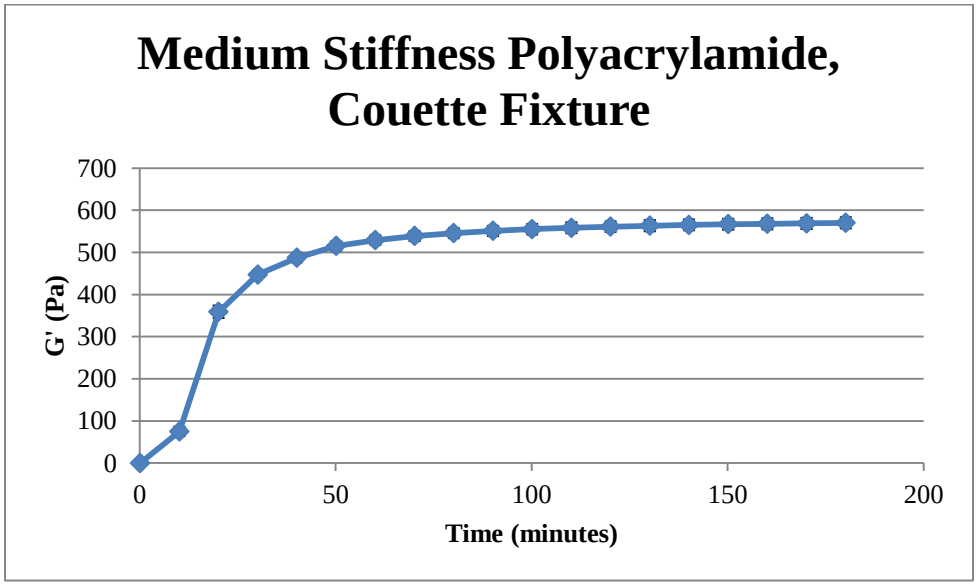

Figure 2.5 Modulus vs. time for medium stiffness polyacrylamide. Material was loaded into coquette fixture and data was collected throughout polymerization. Error bars represent standard error, n=5

Our synthesis methods originated from a well reported methodology [111]. From our stiffness verification, we have found a discrepancy in reported data for

polyacrylamide gel stiffnesses. The method we followed reports the stiffnesses of these gel compositions as 140, 1050, and 60,000Pa. They do not appear to have performed their own modulus measurements, but instead cite Yeung et al. 2005. However, the moduli reported do not match the moduli measured in the reference. Our data does support the moduli reported by Yeung et al. [1]. Figure 2.6 shows their data in black with ours overlaid in red, corresponding to the appropriate acrylamide/bis-acrylamide ratios of the gel recipes.

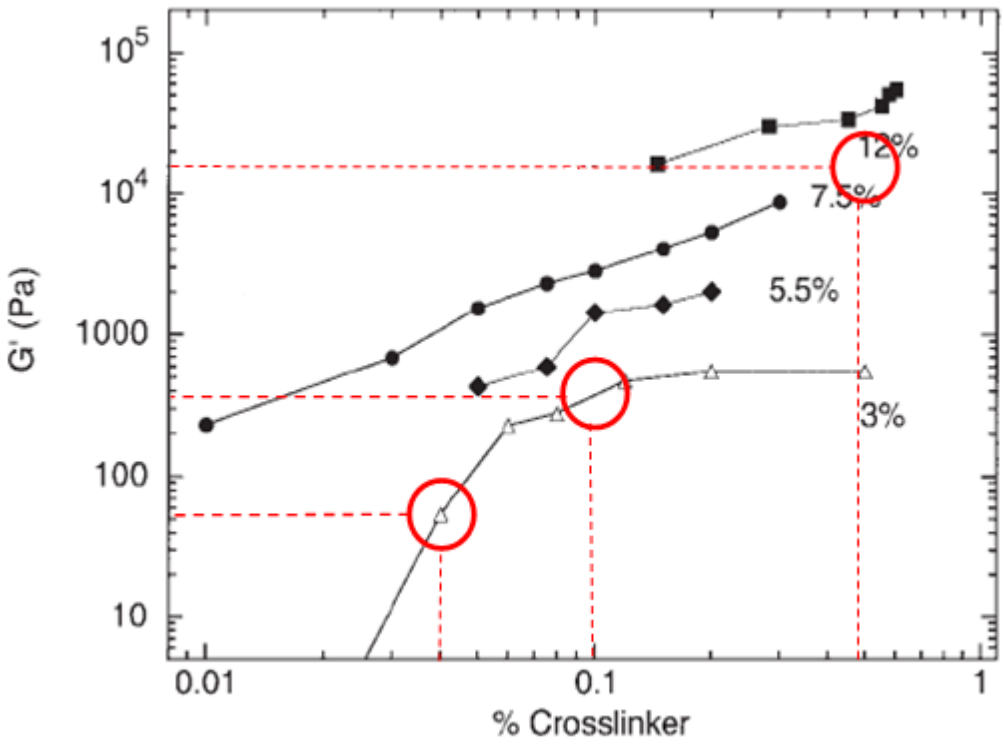

Figure 2.6. Elastic Modulus of Polyacrylamide with a range of acrylamide to bis-acrylamide proportions. Data in black was reported by Yeung et al 2005. Graph shows modulus (G'), expressed in Pascal, vs. % crosslinker, or bis-acrylamide. Individual data lines represent different amounts of acrylamide. Our data is overlaid in red for sake of comparision. (Figure modified from Yeung et al. 2005 [1])

Collagen Quantification: Although gels were functionalized with known amounts of collagen (0.1, 0.2, and 0.4 mg/mL), the amount of protein that efficiently binds to the Sulfo-SANPAH crosslinker is unknown. The density of collagen on the surface of the gel was measured by digesting the collagen with collagenase I and examining the digest products through SDS-PAGE. Collagenase is one of very few enzymes capable of cleaving the native collagen molecule [112]. Collagenase cleaves the triple-helix collagen molecule 25% of the length from the C-terminus, creating two fragments known as TCA (3/4) and TCB (1/4) fragments [113]. The molecular weight of Collagenase Type I used in this study is 110kDa. The TCA fragment is approximately 104 kDa and the TCB fragment, 34 kDa. Because the molecular weight of the TCA fragment is difficult to distinguish from the collagenase itself, quantification was focused on the TCB fragment. Collagen I is composed of three chains: 2 α(I) chains and 1 α(II) chain. When cleaved with collagenase, TCA and TCB fragments will appear as a doublet on a PAGE gel, due to the slight difference in α(I) and α(II) molecular weight.

In order to visualize TCB fragments, collagenase digest products were run on a 10% polyacrylamide gel. Figure 2.7 shows a representative gel for both the standard curve and the experimental samples. On gel A, there is a lane for a collagenase digest sample (collagen + collagenase + sample buffer) and whole collagen (collagen + sample buffer) for comparison. The zero point of the standard curve should not result in any visible bands; however, as seen in Figure 2.7, there is a band at the expected TCB fragment MW. While the zero sample should only contain HEPES, collagenase, $CaCl_2$, EDTA, and sample buffer, there seems to be collagen, and thus collagenase digest

products, present. This issue is still being addressed. Due to issues with the zero point of the standard curve and time constraints, the collagen density has not yet been quantified.

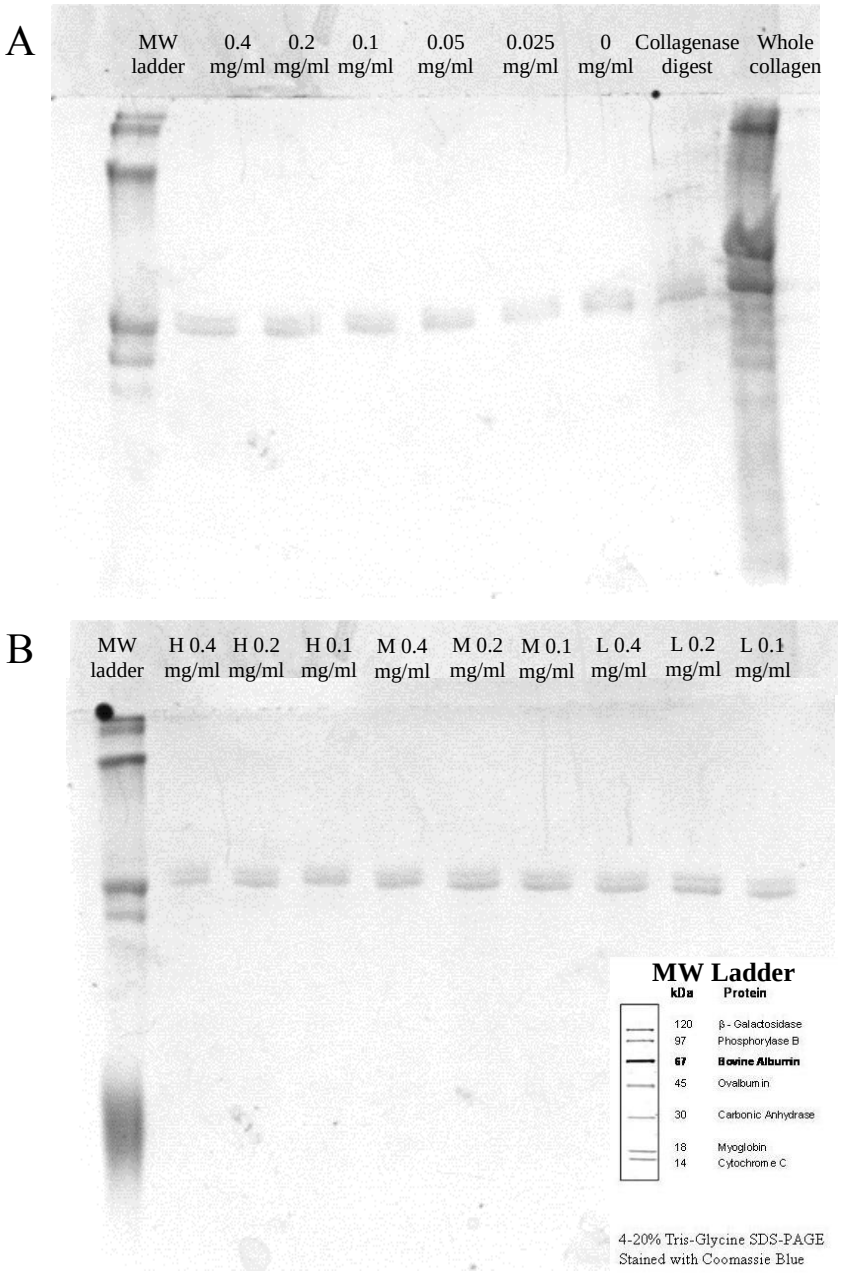

Figure 2.7. SDS PAGE for collagen concentration. 10% polyacrylamide gels were used to resolve the TCB fragment (34kDa). (A) shows the standard curve, plus a collagen digest control and whole collagen. (B) shows bands for each experimental sample.

Despite complications, the method presented above should be suitable to determine the collagen density on polyacrylamide samples. The issue of the zero standard will need to be addressed before densiometric analysis can be performed. Before the collagenase method was selected, several other methods of quantification were attempted. A colorimetric Sirius Red assay, typically used to quantify collagen in histological samples, was attempted. The polyacrylamide substrates absorbed the dye making it impossible to distinguish between actual collagen and background from the polyacrylamide. A similar approach to Reinhart-King 2003 was taken to dissociate the collagen from the substrate using concentrated sodium hydroxide [114]. Following this treatment, collagen agglomerated into a gel-like mass, making accurate pipetting and further analysis impossible.

C17.2s on Polyacrylamide Gels: C17.2s were cultured through 21 days on experimental materials. Following 14 days below 1% total serum, cells were fixed and immunocytochemically stained for marker proteins of interest. Samples of each stiffness, were stained for nuclei, nestin, and β-tubulin III, a neuronal marker, to assess cell fate. Expression of β-tubulin III indicates differentiation of the C17.2 neural stem cells into post-mitotic neurons. When cultured on control materials (glass or collagen coated glass), cells would often sheet off of substrates, which could indicate differences in cell behaviors such as proliferation and differentiation on the different substrates.

When cells were fixed after 21 days of serum withdrawal (14 days below 1%), few cells remained on the culture substrate. Cells are very delicate at this point and may have been dislodged during changing of media or during the fixation process. During the

most recent experiment, cells were fixed after 14 days of serum withdrawal to ensure that cells were still present of the polyacrylamide substrates. Cells were stained for nuclei and β-tubulin III. Phase contrast images of the same field of view as fluorescence images were also captured. Figures 2.8, 2.9, and 2.10 show these images, both fluorescent and phase contrast, of C17.2s cultured on high, medium, and low stiffness polyacrylamide substrates, respectively. Qualitatively, there appeared to be fewer neurons on the high stiffness samples, and those present had shorter and less aligned neurites. From the phase contrast images, cells appeared smaller and closer packed, with few cells with neuronal morphology. There was a visible difference in the number of neurons between the high and medium stiffness samples. Polarized cells with neurite-like extensions can be seen in phase contrast. Neurons appear more aligned in some areas of the culture surface. As expected, neurons on the softest substrate were more in number and neuronal morphology. Neurons were locally aligned with an expansive network of neurites, as seen in Figure 2a, c, and e.

Without additional samples, it is difficult to comment on the effect of collagen concentration on NSC differentiation. Additional experiments would allow for statistical analysis to determine if and how collagen density impacts C17.2 differentiation in combination with substrate stiffness. Furthermore, without accurate quantification of bound collagen density, it is unclear if there is a notable difference between samples of the same stiffness.

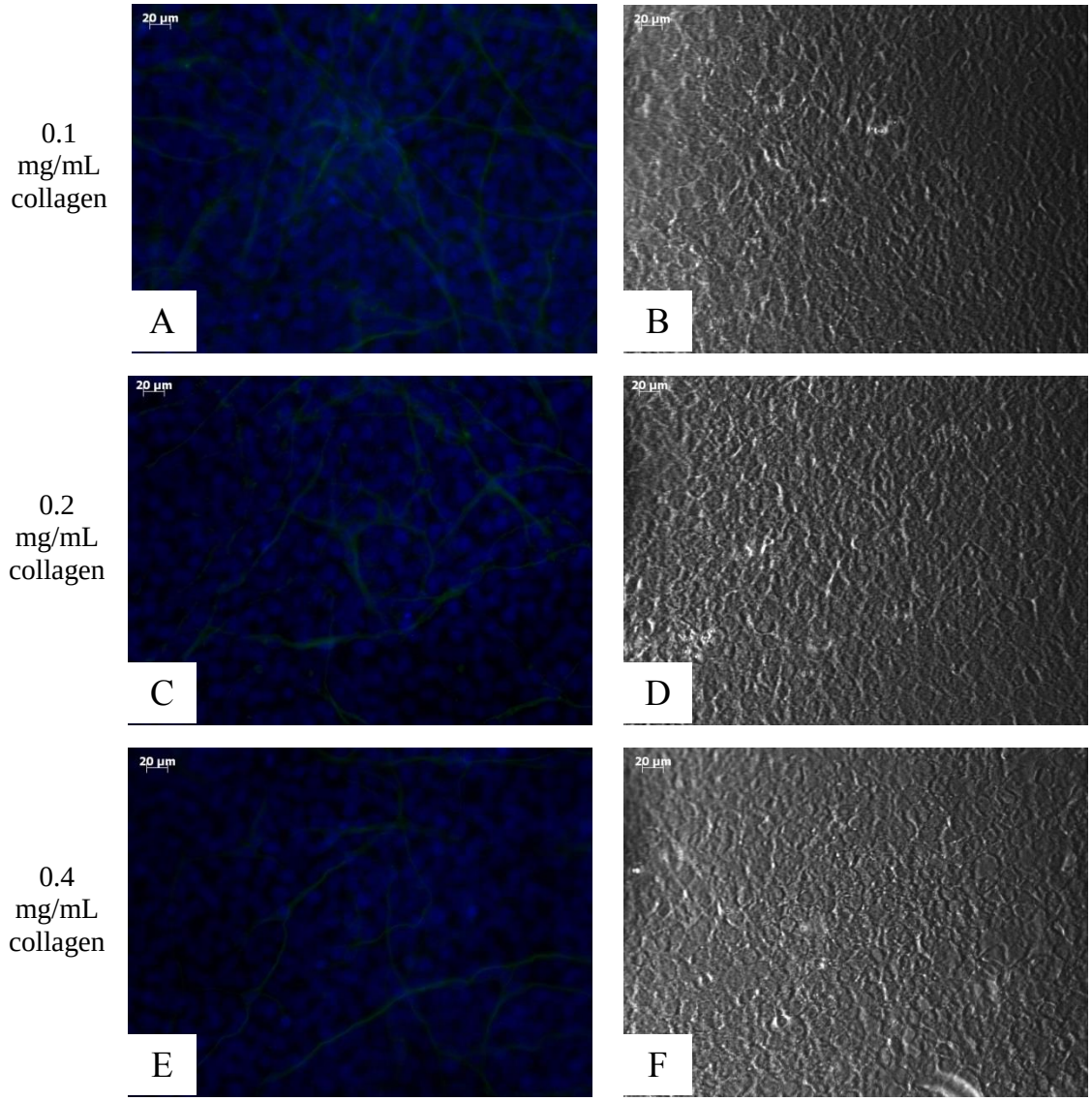

Figure 2.8. C17.2 NSCs were cultured on high stiffness polyacrylamide gels with 0.1 mg/mg (a&b), 0.2 mg/ml (c&d), and 0.4 mg/ml collagen. Following 14 days of serum withdrawal, cells were stained for a neuronal marker, β- tubulin III (green) and nuclei (blue) (a, c, d). Phase contrast images (b,d,f) of the same field of view accompany immunocytochemistry pictures (a,c,e) for reference.

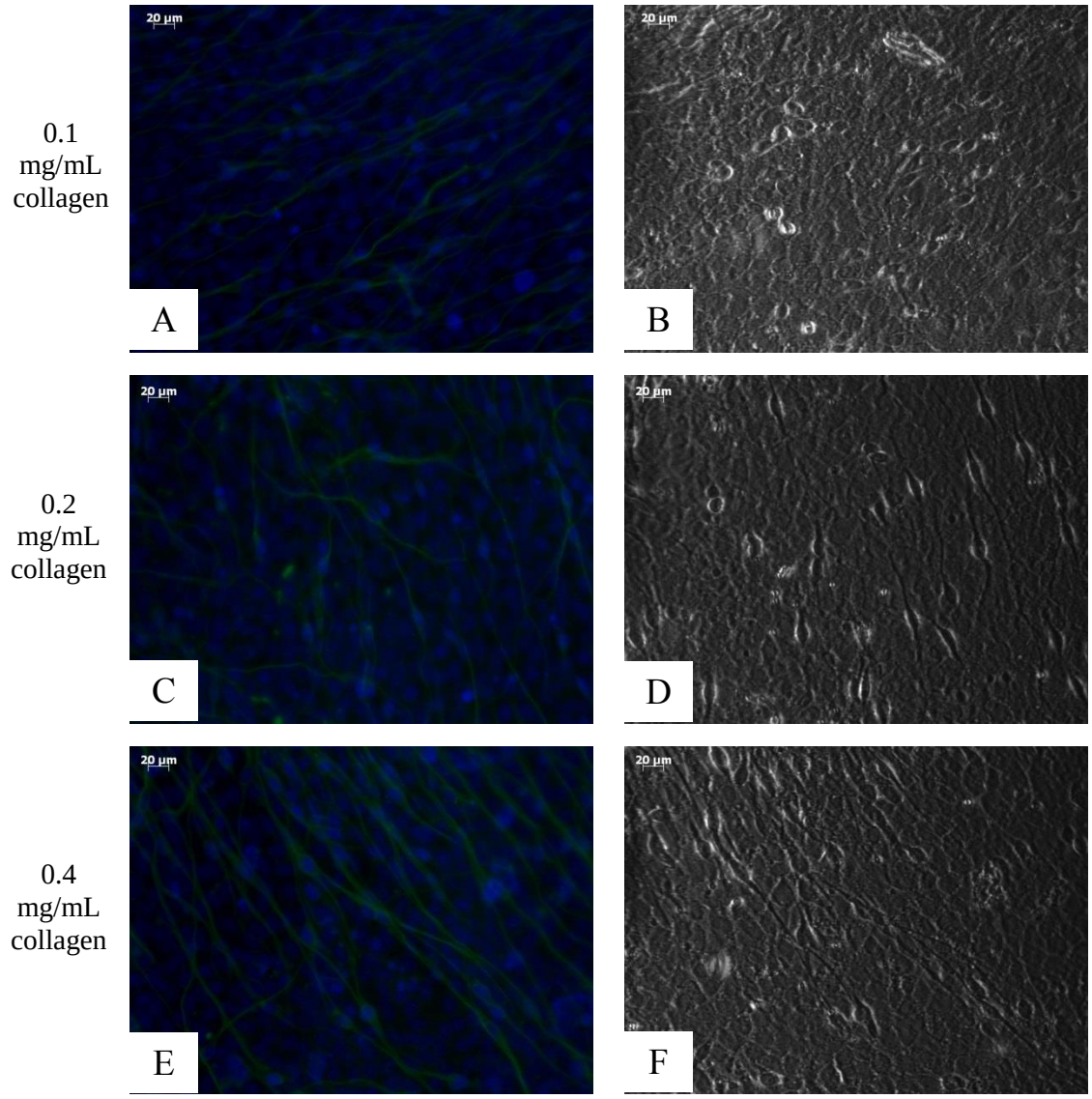

Figure 2.9. C17.2 NSCs were cultured on medium stiffness polyacrylamide gels with 0.1 mg/mg (a&b), 0.2 mg/ml (c&d), and 0.4 mg/ml collagen. Following 14 days of serum withdrawal, cells were stained for a neuronal marker, β- tubulin III (green) and nuclei (blue) (a, c, d). Phase contrast images (b,d,f) of the same field of view accompany immunocytochemistry pictures (a,c,e) for reference.

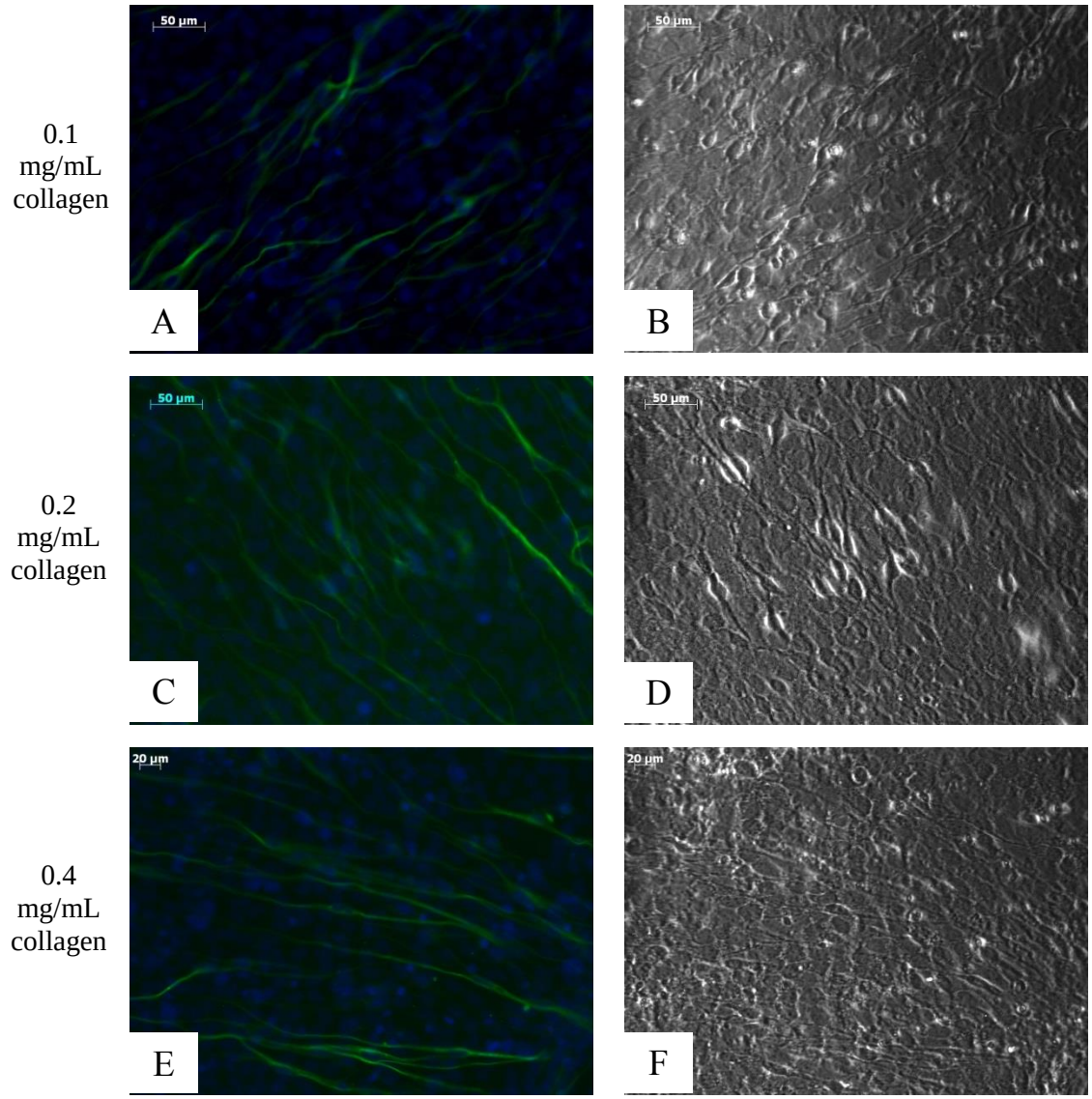

Figure 2.10. C17.2 NSCs were cultured on low stiffness polyacrylamide gels with 0.1 mg/mg (a&b), 0.2 mg/ml (c&d), and 0.4 mg/ml collagen. Following 14 days of serum withdrawal, cells were stained for a neuronal marker, β- tubulin III (green) and nuclei (blue) (a, c, d). Phase contrast images (b,d,f) of the same field of view accompany immunocytochemistry pictures (a,c,e) for reference.

Conclusion

In this study, I have provided valuable characterization of material substrates used to investigate the effects of chemo-mechanical factors on neural stem cell differentiation.

Substrate stiffness was verified, and found to support values published by Yeung et al. [1]. A discrepancy in the literature was discovered; the method we followed erroneously cites stiffness values from Yeung et al. Additionally, a method to determine the amount of collagen functionalized to the polyacrylamide gels by the crosslinker Sulfo-SANPAH was developemd. This information will allow for better control of biochemical modification of polyacrylamide surfaces, expanding the value of the polyacrylamide platform. Additional studies are required to confirm collagen density on the polyacrylamide gels, as well as its effect on NSC differentiation. Future samples should be fixed after 14 days of serum withdrawal to prevent loss of cells during the final week.

Future work for this experiment is multi-fold. To continue on the work performed by Colleen Curley, specimens will be assessed for formation of synapses. Synaptogenesis of C17.2s was explored on substrates of various stiffnesses, but has not yet been characterized across various collagen concentrations. Furthermore, as whole ECM proteins such as collagen can be difficult to control, interpret, and reproduce, collagen will be replaced by synthetic peptides. The beginnings of this work will be discussed in Chapter 3. Finally, further analysis of neuronal subtypes, through additional immunocytochemical staining and PCR, will provide insight to the functionality of the mature neurons produced. Results from this work further the knowledge base for the design of biomaterials scaffold to direct neural stem cell fate, with applications in cellular implants for treatment of neurodegenerative diseases.

Chapter 3

Peptide-Functionalized Polyacrylamide Substrates for Neuronal Differentiation

Introduction

The cellular microenvironment influences cellular processes such as adhesion, proliferation, and differentiation [101, 102]. Research has shown that cells can sense and respond to a variety of stimuli, including soluble and insoluble factors (such as proteins and small molecules) and externally applied mechanical stresses. Additionally, cell response to mechanical properties of the cellular environment, such as substrate stiffness, has been suggested to play an important role in cell processes. While both biochemical and mechanical signaling have been explored independently, very few studies have been performed to study well-controlled chemo-mechanotransduction.

NSCs can be used as a model to study cell-ECM interactions associated with the developing neural environment. NSCs can give rise to multiple cell types, including neuronal, astrocyte, and oligodendrocyte lineages, in response to distinct cues [115]. Identifying specific factors in the microenvironment, such as biochemical factors, as well as understanding the effect of matrix stiffness will provide new tools to promote stem cell differentiation into a particular lineage.

In vivo, the intercellular space is filled with a unique assembly of extracellular matrix (ECM) proteins. Cells interact with ECM proteins through integrin receptors in the cell membrane and induce signaling cascades within the cell. During neural development, these extracellular cues can promote differentiation of NSCs into cells of

mature phenotypes [103]. Synthetic scaffolds have been developed to study the effect of immobilized ligands on NSC differentiation [107-110]. These surfaces containing ECM proteins and peptide sequences have been observed to modulate cell fate and function. Peptides containing binding sequences from fibronectin (AYAVTGRGDSPASA), laminin (ADPGYIGSRGAA), and EGF repeats from laminin and tenascin (ANDNIDPNAVAA) are used in this study, due to their known presence in the developing neural environment [88, 116-118].

While activation of signal transduction pathways by interaction of integrins and bioactive peptides has been well studied, physical properties of the microenvironment also play a role in stem cell differentiation [11, 21]. Matrix elasticity has been observed to direct stem cell lineage specification. For example, human mesenchymal stem cells have been reported to differentiate into various cell types including neurons, myoblasts, and osteoblasts, depending on the culture substrate stiffness [3]. Neural stem cell responses to substrate stiffness are less well-defined, and highly dependent upon cell type chosen [108, 119].

With regards to proliferation and differentiation of stem cells for therapeutics, a chemo-mechanical approach may have profound effects on potential clinical translation. The roles of both biochemical and mechanical signaling in fate modification of neural stem cells have been explored independently. Polyacrylamide gels of varying stiffnesses within the range of soft tissue can be synthesized by adjusting the ratio of acrylamide:bis-acrylamide, thus adjusting the degree of crosslinking. As the degree of crosslinking increases, the Young's modulus also increases. Peptides that have been shown to impact

neuronal development [88] are covalently linked to the substrate to promote neuronal differentiation. This material substrate allows for independent control of biochemical signals and mechanical signals for the *in vitro* study of the combinatorial effects of chemo and mechanical signaling on neural stem cell differentiation.

This study develops a platform to study the combination of these factors. To address the optimization of peptide functionalization, a single stiffness of PA was the focus. Peptides were individually crosslinked to the PA and the critical concentration was determined using a cell based assay. Using the data collected in this study, a more complex platform involving combinations of peptides and gels of different stiffnesses will be used to direct differentiation of NSCs.

Materials and Methods

Peptide Synthesis: The peptides, listed in Table I, were synthesized using standard FMOC solid state synthesis on an Intavis Res-Pep synthesizer using Fmoc - Ala - HMP - TentaGel resin (Anaspec). FMOC protected amino acids were added to the peptide chain using the activating reagent 2-(1H-benzotriazol-1-yl)-1,1,3,3-tetramethyluronium hexafluorophosphate (HBTU). Upon the addition of the N-terminal amino acid, the protection group was removed under 20% piperidine deprotection conditions. Cleavage from the resin and additional side chain protection groups was performed with 88% trifluoroacetic acid with 2% triisopropylsilane as a scavenger molecule. Following cleaving, peptides were ether precipitated and dried. A HPLC purified RGD peptide

(GRGDSP) was purchased (Bachem) as a control. ESI-mass spectrometry analysis was used to confirm the expected m/z ratio of the peptides.

3 Letter Name	Sequence	Shortened Sequence	Origin	Function
RGD	AYAVTG**RGD**SPASA	G**RGD**SPA	Fibronectin type III repeat	Adhesion, synapse formation [116]
YIG	ADPG**YIG**SRGAA	G**YIG**SRA	Laminin	Adhesion, synapse formation [117]
NID	AND**NID**PNAVAA	ND**NID**PNAVAA	Laminin, tenascin	Basement membrane organization [118]

Table 3.1: Peptides chosen for study based on work by Jedlicka et al. [88] Bold amino acids indicate cell binding sequences.

Polyacrylamide Gel material synthesis: Polyacrylamide (PA) gels were prepared according to the method of Yeung et al. [1]. Briefly, glass coverslips (VWR) were coated with a thin coating of (3-aminopropyl) trimethoxysilane. Coverslips were then washed with ddH_2O and subsequently incubated in 70% glutaraldehyde (in 1X PBS) for 30 minutes at room temperature. Coverslips were washed again in ddH_2O, dried, and used immediately or stored for up to several weeks in a dry place. Precursor solutions were made from acrylamide (40% in ddH_2O), N,N'-methylenebisacrylamide (2% in ddH_2O), and HEPES (0.5M, pH 4.22). To create a low stiffness gel, 75 μL 40% acrylamide, 20 μL 2% bis-acrylamide, 100 μL 0.5M HEPES, 0.5 μL TEMED, and 648.9 μL ddH_2O were combined and degassed for 30 minutes [111]. Following degassing, ammonium persulphate was added to a final concentration of 0.05%. The acrylamide solution was then pipetted onto each activated coverslip and topped with a coverslip (modified to prevent adherence to the gel). The gels were allowed to polymerize and used immediately or stored in HEPES (50mM, pH 8) for up to two weeks.

Peptide Functionalization: Extracellular matrix were conjugated to the gel using N-Sulfosuccinimidyl-6-(4'-azido-2'-nitrophenylamino) hexanoate (Sulfo-SANPAH). Functionalization was performed two ways. In the first method, 100μL of the sulfo-SANPAH solution (0.5 mg/mL in HEPES, pH 8.0) was pipette onto each gel surface. The gels were then placed several inches under an ultraviolet (UV) lamp and irradiated for 15 minutes. The samples were then washed thoroughly with 50mM HEPES (pH 8). The peptides and/or proteins were then added onto the activated polyacrylamide and incubated for 4 hours under UV at RT (collagen I: 0.2mg/ml, peptides: 10nmol/cm^2). In the second method, the peptide was bound to the sulfo-SANPAH before it was crosslinked to the gel. Peptide aqueous solution was added into Sulfo-SANPAH (0.5mg/mL) solution with a molar ratio of 10:1. The peptide-sulfo-SANPAH complex was then added to the gel surface, crosslinked using UV, and rinsed with 50mM HEPES. Following failed attempts with full length peptides, peptide sequences were truncated to allow for more effective binding.

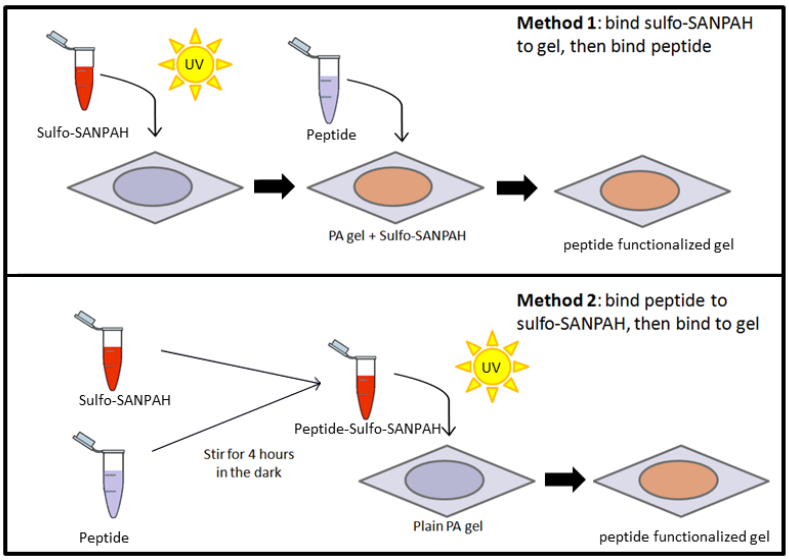

Figure 3.1. Schematic of methods used for peptide functionalization of PA with Sulfo-SANPAH

Cell Culture: C17.2 neural stem cells, obtained from Dr. Evan Snyder at the Burnham Institute, were maintained in high-glucose DMEM containing 10% FBS, 5% horse serum, and 2mM L-Glutamine. Cells were passaged at 80-90% confluency using cell stripper. To confirm the presence of peptide on the gels, cells were seeded on the same experimental materials at a density of 10,000 cells/cm^2. Without peptide present, cells will not adhere to PA. Cells were imaged using phase contrast microscopy to assess adherence to the PA substrates.

Results and Discussion

Peptide Analysis: Electrospray ionization-mass spectrometry was used as confirmation of expected m/z ratios of synthesized peptides. A Q-Trap 3200 instrument (ABSciex) was used for the analysis. A representative spectrum for the shortened RGD sequence (GRGDSPA) is shown in Figure 2.

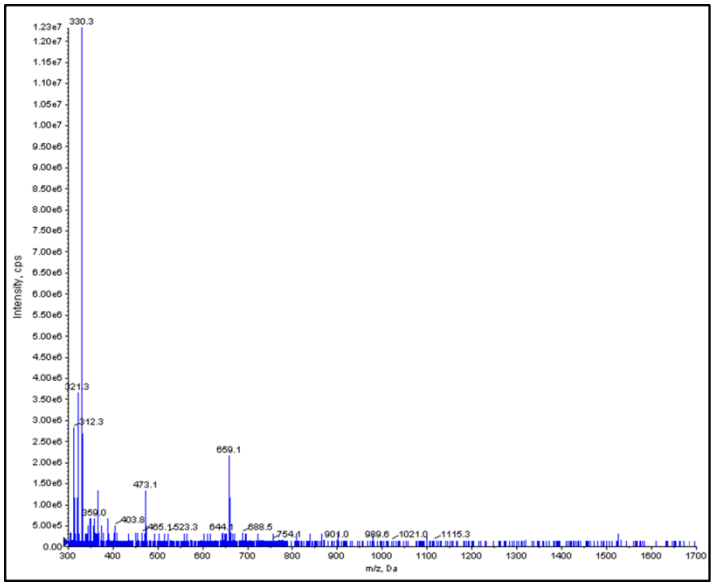

Figure 3.2. Electrospray Ionization-Mass Spectrometry Spectrum for in-house synthesized RGD (expected MW=658.3)

Cellular Adherence on PA Gels: Without peptide or protein functionalization, cells will not adhere to PA gels. PA was functionalized with varying concentrations of peptide, ranging from 1-200 nmol/cm^2, to determine the amount of peptide necessary for cellular

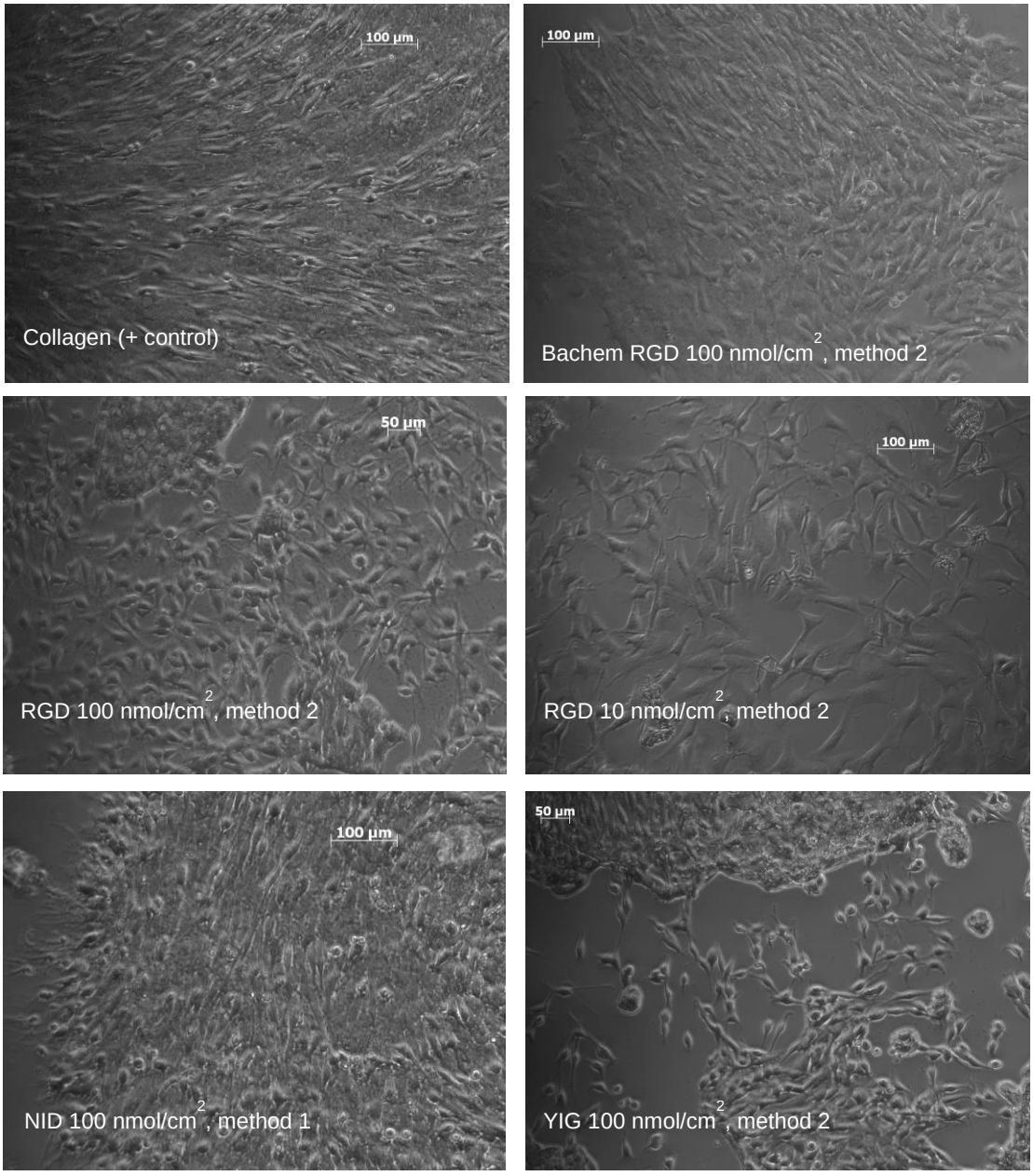

Figure 3.3. C17.2 NSCs were cultured on PA gels functionalized with varying concentrations of peptides to determine the critical peptide concentration for cell adhesion.

adhesion. Both methods of Sulfo-SANPAH crosslinking were used for comparison. Cells were cultured on functionalized PA for 4-6 days and phase contrast images were visually assessed for adherent cells. Representative images of adherent cells are shown in Figure 3.3. Table II summarizes the extent of cell adhesion on the experimental materials. Cells

did not adhere to materials with peptide concentrations less than 100 nmol/cm^2. Only a select few samples showed cell growth comparable to collagen, the positive control; those specimens are denoted as "+ +" in Table 3.2.

Concentration (nmol/cm^2)	Method	Bachem RGD	RGD	YIG	NID
1	1		- -		
10	1		-		
100	1	-	+	+	+
1	2	--	--	--	--
10	2	-	-	-	-
100	2	+ +	+ +	+ +	+
200	2	+	-	+	+

Table 3.2. Summary of NSC adherence on PA gels functionalized with varying concentrations of peptide. (- - = minimal cell adhesion, - = cell spheres present, + = mix of adherent cells and spheres, + + = majority of cells adhered)

Conclusion

From the results of the cell adhesion experiment, it appears that C17.2 NSCs adhere best to PA functionalized with peptides at 100 nmol/cm^2. Method 2 of Sulfo-SANPAH crosslinking provided fewer cell spheres and more adherent cells. Further experiments using X-ray photoelectron spectroscopy will be performed to determine the amount of peptide bound to the PA following functionalization. Additionally, atomic force microscopy will be used to confirm that there are not major nanotopographical differences between functionalized and unfunctionalized PA gels.

Cell fate can be mediated by both mechanical and chemical substrate properties. In this study, a platform for studying how these properties impact cell fate was designed

and optimized. This platform combines the chemical and mechanical cues of the platform discussed in Chapter 2, while providing more control and versatility in peptide functionalization. Peptides can be tailored to the cells and phenotype fate desired. Moving forward, this material platform will be used to further study the combinatorial roles of surface chemistry and elastic modulus in NSC differentiation.

Chapter 4

Physical and Biological Characterization of PEGylated Peptide Modified Silica Nanoparticles

Introduction

Cellular membranes contain surface receptors capable of detecting extracellular signaling molecules. Activation of these cell membrane receptors triggers signal transduction pathways that may alter cell migration, differentiation, and other events. Nanomaterials, such as nanoparticles, have been researched for use in nanomedicine, however, little is currently known about the way nanomaterials interact with cellular receptors. The objective of this work is to design, synthesize, and characterize novel nanomaterials to investigate ligand-receptor binding. In the study that will be presented, peptide functionalized PEGylated silica nanoparticles are conjugated with molecules that mimic the natural receptor ligand in order to provide selective targeting to integrin receptors of interest. Silica nanoparticles with a narrow particle size distribution were synthesized by hydrolysis of tetraethylorthosilicate in an aqueous L-lysine solution. This method is more benign (lower pH) than the traditional Stöber process, allowing for the addition of bioactive peptides. Nanoparticle size and morphology were characterized using transmission electron microscopy (TEM). RGD, a 10-mer peptide containing Arg-Gly-Asp from fibronectin type III, was synthesized using 9-fluorenylmethyloxycarbonyl (Fmoc) solid state synthesis. Peptide molecules are further modified with polyethylene-glycol bis(amine), molecular weight 10,000, to be

used as a flexible spacer, through crosslinking with 1,5-Difluoro-2,4-dinitrobenzene. PEGylated-peptide molecules are then linked to (3-aminopropyl)trimethoxysilane (APTMS) to allow conjugation to the silica nanoparticle. Nanoparticle surfaces are decorated with the APTMS-PEG-peptide at a density of 1:1000 peptides per PEG. Peptide functionalized PEGylated nanoparticles were characterized using TEM, Fourier Transform Infrared Spectroscopy (FTIR), thermogravimetric analysis (TGA), and *in vitro* cell analysis.

Materials and Methods

Peptide Synthesis: An RGD peptide (AYAVTG**RGD**SPASA) was synthesized using standard FMOC solid state synthesis on an Intavis Res-Pep synthesizer using Fmoc - Ala - HMP - TentaGel resin (Anaspec). FMOC protected amino acids were added to the peptide chain using the activating reagent 2-(1H-benzotriazol-1-yl)-1,1,3,3-tetramethyluronium hexafluorophosphate (HBTU). Upon the addition of the N-terminal amino acid, the protection group was removed under 20% piperidine deprotection conditions. Cleavage from the resin and additional side chain protection groups was performed with 88% trifluoroacetic acid with 2% triisopropylsilane as a scavenger molecule. Following cleaving, peptides were ether precipitated and dried.

Nanoparticle Synthesis: Silica nanoparticle sols were synthesized as described by Fan et al. 2008 by hydrolysis of TEOS (98%, Aldrich) in aqueous solutions of the basic amino acid *L*-lysine (Sigma-Aldrich), illustrated in Figure 4.1 [120]. A 5.84mM solution of L-Lysine was prepared in ddH20, heated to 90°C for 20 minutes, then cooled to room

temperature. TEOS was added gradually over 48 hours under magnetic stirring at 750 rpm.

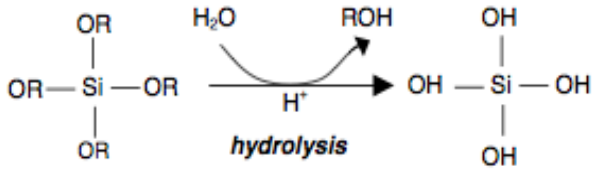

Figure 4.1. Sol-gel reaction. The alkoxysilane, TEOS in this case, is hydrolyzed to form reactive –OH groups. Silanol groups are then condensed to form a connective silica network.

PEG-silane precursors were prepared by methods outlined by Cauda, et al. [91]. Briefly, 6.0 mmol of PEG-MW8000 in 10 mL THF were added to 40mL 0.5M NaOH and stirred for 1 h at 0 °C. Then 10mL 0.7M *p*-toluenesulfonyl chloride in THF was added drop over 1 hour at 0 °C and stirred for 3 additional hours. The solution was poured onto 20 mL 1 M HCl and the organic solvent was evaporated. The residue was extracted 3 times with chloroform and the organic phase was dried over $MgSO_4$, filtered and the solvent was evaporated. The product was reacted with 1.40 mL aminopropyl triethoxysilane(APTES) in 25 mL chloroform at 70 °C for 8 hours. The organic solvent was then evaporated and the final product collected. The chemical reactions are outlined in Figure 4.2.

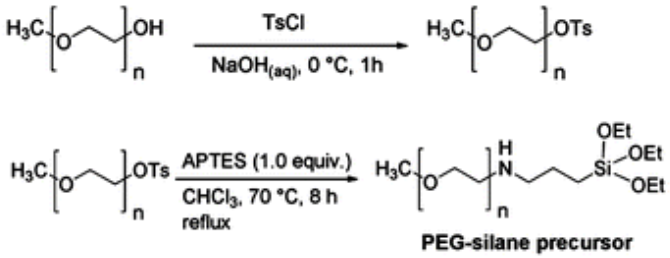

Figure 4.2. The two reactions used to synthesize the PEG-silane precursor [91].

RGD peptide was conjugated to PEG-bis-amine-MW10,000 through cross-linking with 1,5-Difluoro-2,4-dinitrobenzene. The structure of the RGD peptide is shown in Figure 4.3. DFDNB was again used to attach a silane group (APTMS) to the other amine end of the PEG molecule. Figure 4.4 shows a schematic of the assembled complex. Based on the size of the precursors, the entire complex should be approximately 12 kDa.

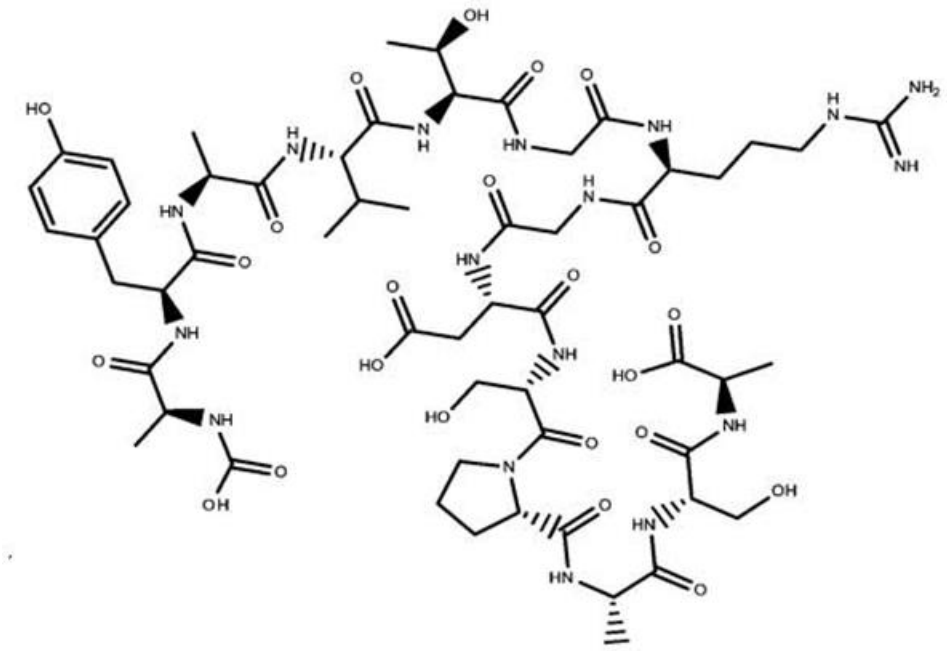

Figure 4.3. Structure of AYAVTG**RGD**SPASA peptide.

Figure 4.4. Schematic of assembled PEG-peptide complex. DFDNB is used as a crosslinker to link the peptide to PEG and PEG to a silane to allow for further binding with the silica NPs. (not to scale)

Nanoparticles were decorated with plain PEG-MW8,000 (1 mole% PEG-silane:silica) and RGD-PEG-MW10,000 (0.001 mole% PEG-RGD:silica) through a delayed co-condensation reaction. NPs were fluorescently labeled with fluorescein isothiocyanate-silane to aid in visualization. 1.0 mg fluorescein isothiocyanate was stirred for 30 min at room temperature with 5.0 µL 3-aminopropyltrimethoxysilane (APTMS) in 500.0 µL anhydrous DMF [121]. PEGylated silica NPs with and without peptides were synthesized using a delayed co-condensation reaction [91]. NPs were purified using dialysis in dH_2O for cell culture and characterization studies.

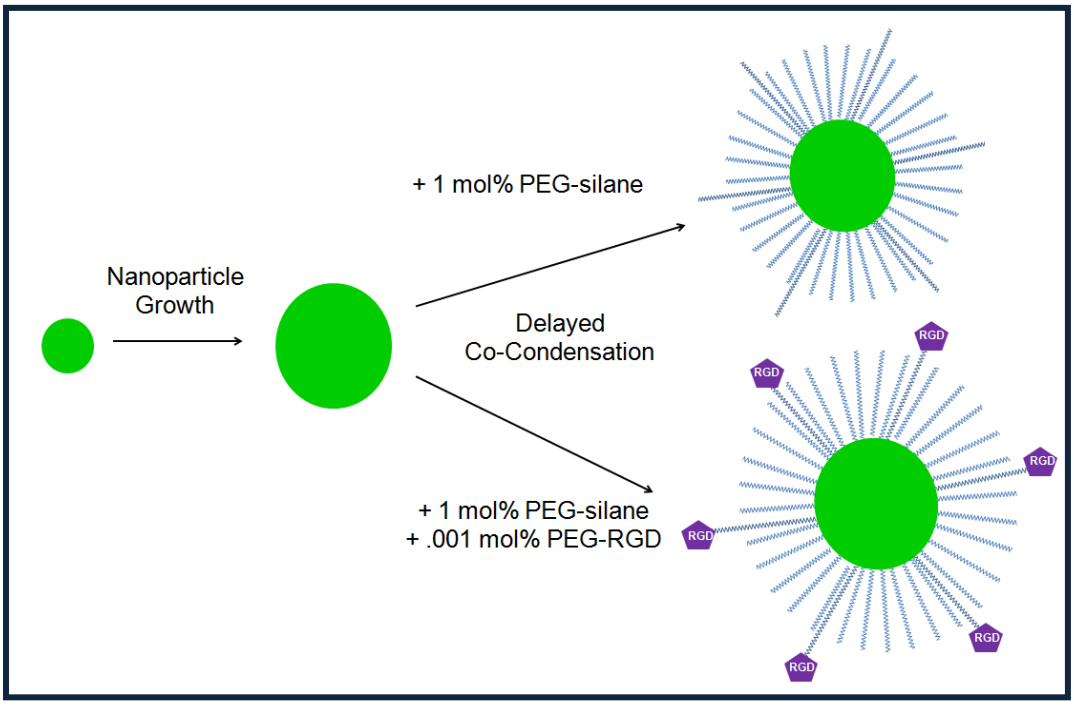

Figure 4.5. Schematic of PEGylated nanoparticle synthesis. Nanoparticles are formed by a nucleation and growth reaction. PEG-silane and PEG-RGD are added through a delayed co-condensation reaction.

Nanoparticle Characterization: Nanoparticles were imaged using a JEOL 2000FX Transmission Electron Microscope at 200kV. NPs were observed for size, homogeneity, and apparent morphology. Chemical bonding within nanoparticle structures was analyzed using Fourier Transform Infrared Spectroscopy. A Perkin-Elmer FTIR Spectrum 100 was used to verify bonding of PEG and confirm chemical bonding within NPs. Thermogravimetric analysis was performed from 0 to 800°C using a TA Insruments Q500 Thermogravimetric Analyzer to verify presence of PEG and peptide. Finally, a short-term *in vitro* cell experiment was used to visualize interaction between c17.2 neural stem cells and nanoparticles. Dilute NPs in dH_2O were added to sub-confluent C17.2s and observed with phase contrast and fluorescent microscopy over 2 hours.

Results and Discussion

Transmission Electron Microscopy: Visualization of nanoparticles with TEM revealed spherical particles on the order of 100-200nm, shown in Figure 4.5. The population is not entirely homogenous in size, though all particles appear to be spherical. No significant size difference was observed between samples, though surface morphology appears rougher in (b) and (c). We expected to observe ~5-10nm increase in PEGylated NP diameter due to addition of PEG molecules. Minimal size difference was observed between samples, perhaps due to dehydration for TEM visualization or volume exclusion properties of PEG.

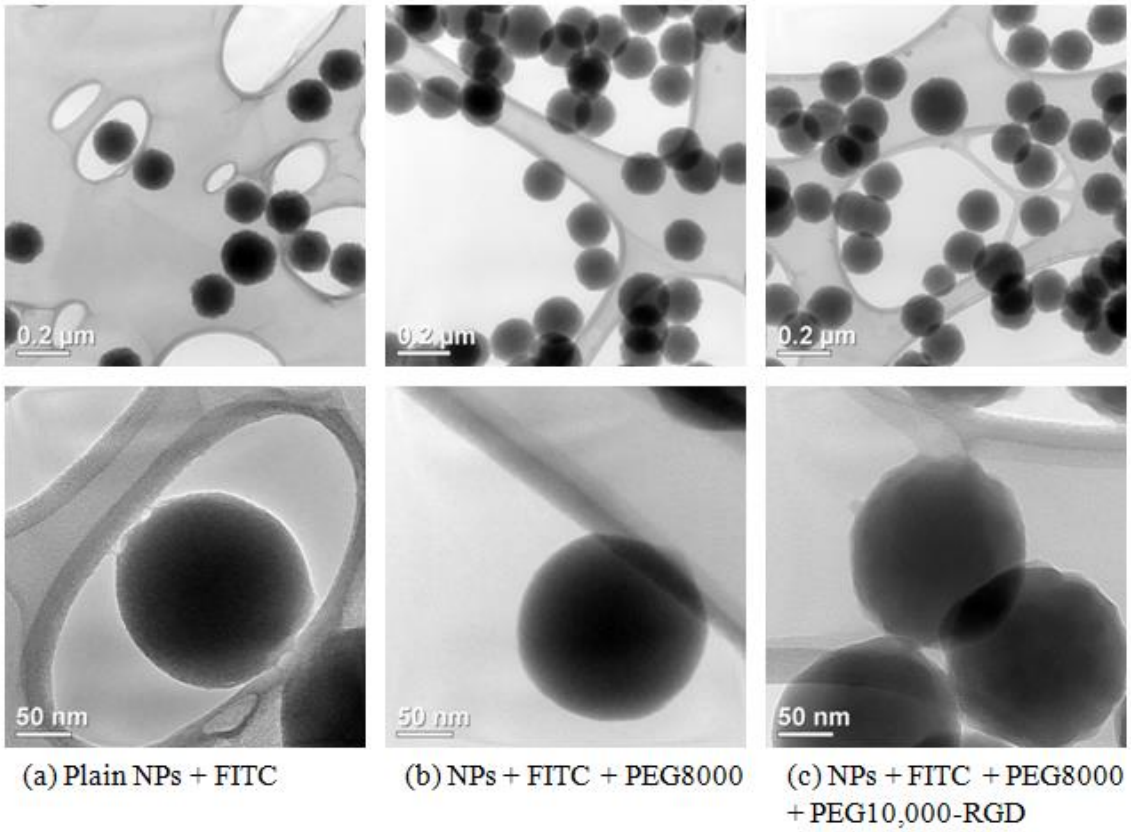

Figure 4.6. Representative TEM micrographs of the three NP populations (a) Plain NPs + FITC, (b) NPs + FITC + PEG8000, and (c) NPs + FITC + PEG8000 + PEG10,000-RGD

Fourier Transform Infrared Spectroscopy: FTIR was performed to verify chemical bonding within the nanoparticle structures. Specifically, we were looking to confirm the presence of PEG within the system. C-H stretching modes of -CH3 and -CH2 groups of the PEG chain were observed at 2900cm^{-1}. Changes were seen in the 1350-1450cm^{-1} range, indicative of deformation vibrations of the PEG backbone. The C-N stretch mode is of particular interest to confirm the presence of peptide within the complex. However, the signal due to the bands of the SiO_2 framework mask any other signal in the 1000-1200cm^{-1} range, making it impossible to confirm peptide binding.

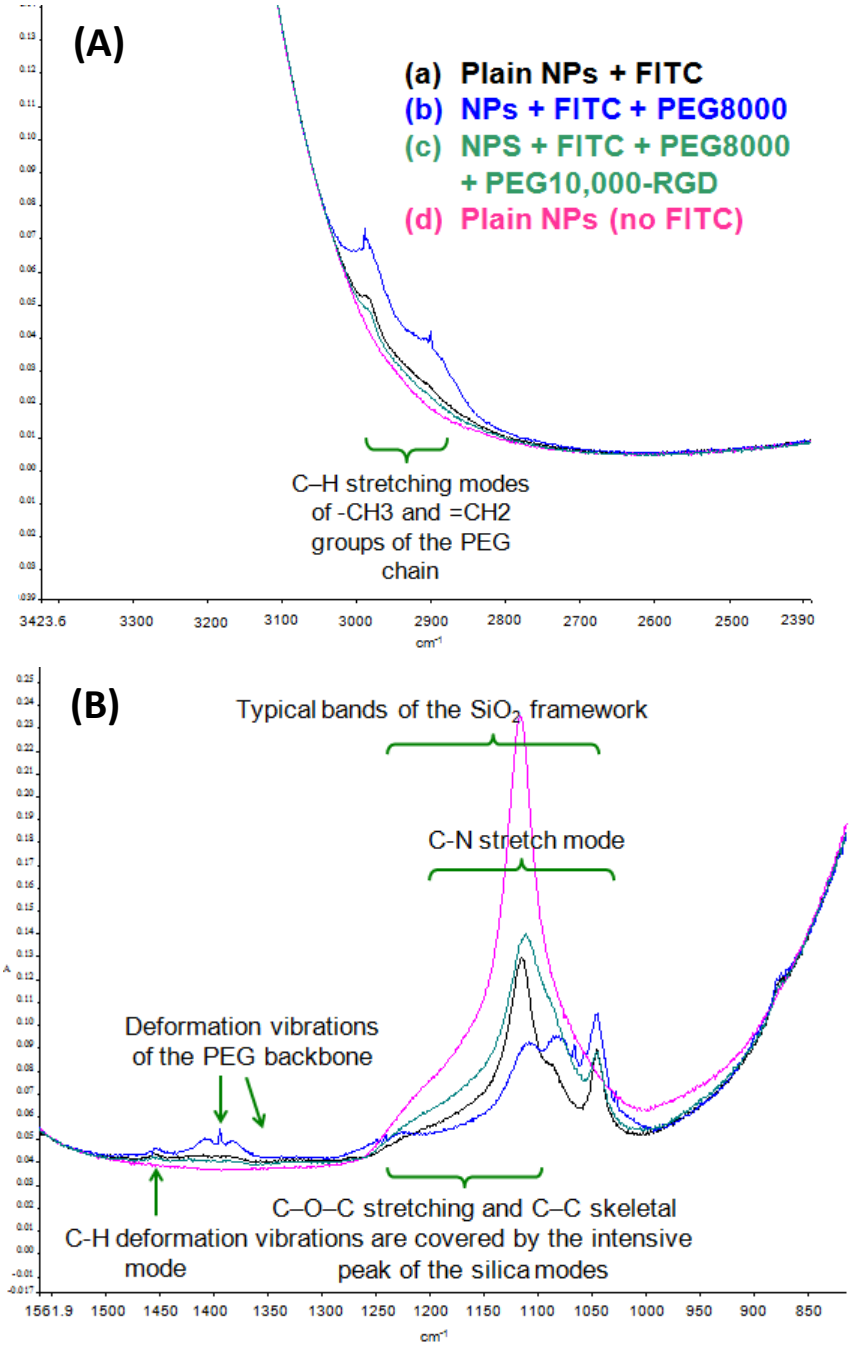

Figure 4.7. FTIR spectra of four populations of NPs: (a) Plain NPs + FITC, (b) NPs + FITC + PEG8000, (c) NPs + FITC + PEG8000 + PEG10,000-RGD, and (d) Plain NPs (No FITC).

Thermogravimetric Analysis: Thermogravimetric analysis is a technique in which physical properties and measured as a function of temperature. Often used to observe phase transitions and chemical phenomena, we made use of technique to observe the

decrease in weight with rising temperature. Since PEG and the peptide will deteriorate at lower temperatures than the silica NP, this method can be used to confirm the presence of these species. The results in Figure 4.7 show an initial loss of physisorbed water below 200°C. From 200 to 400°C, the organic groups are lost, resulting in a difference in weight between PEGylated and plain NPs. The plain sample exhibits some weight loss, attributed to the residual ethoxy groups formed during synthesis [91]. Both PEGylated samples show evidence of similar amount of bound PEG, seen in the similar weight loss of both samples. However, it cannot be confirmed from this analysis that there is peptide present in the sample.

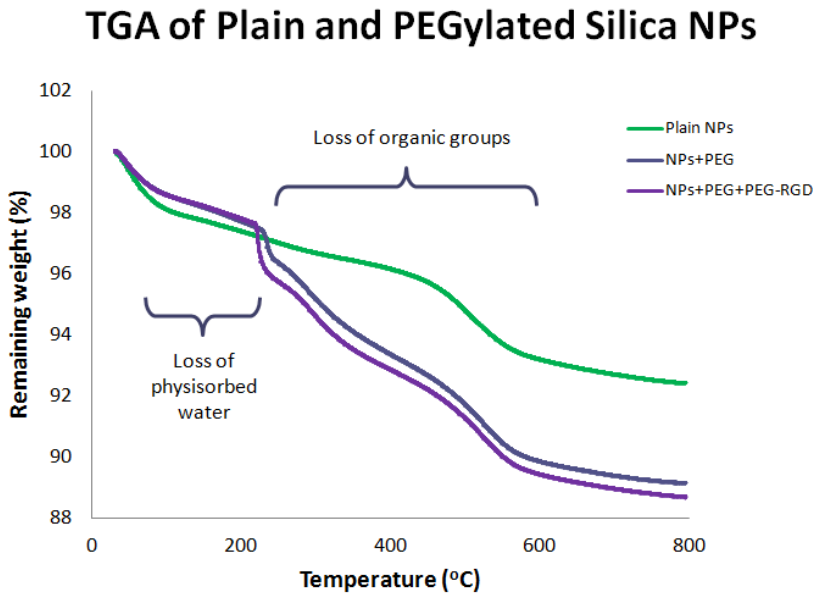

Figure 4.8. Thermogravimetric analysis of unfunctionalized and PEGylated NPs: (green) Plain NPs, (blue) NPs + PEG8000, and (purple) NPs + PEG8000 + PEG10,000-RGD

***In Vitro* Cell Analysis:** Nanoparticles were dialyzed and diluted in H_2O and added to cultures of sub-confluent C17.2 NSCs. NP-cell interactions were observed over a 2 hour period by fluorescent and phase contrast microscopy. Figure 4.8 shows representative images of each NP type in contact with cells. Particle agglomeration was observed in all samples, though more so in (a) and (b). NP clusters are on the order of 1μm. C17.2 cells survive exposure to all NP samples, at least in the short term. Cells appear more spread with (c) PEGylated-RGD NPs than with (a) plain or (b) PEGylated NPs. This result is expected based on the known functions of the RGD peptide. NP-cell interactions will be further investigated using higher resolution microscopy

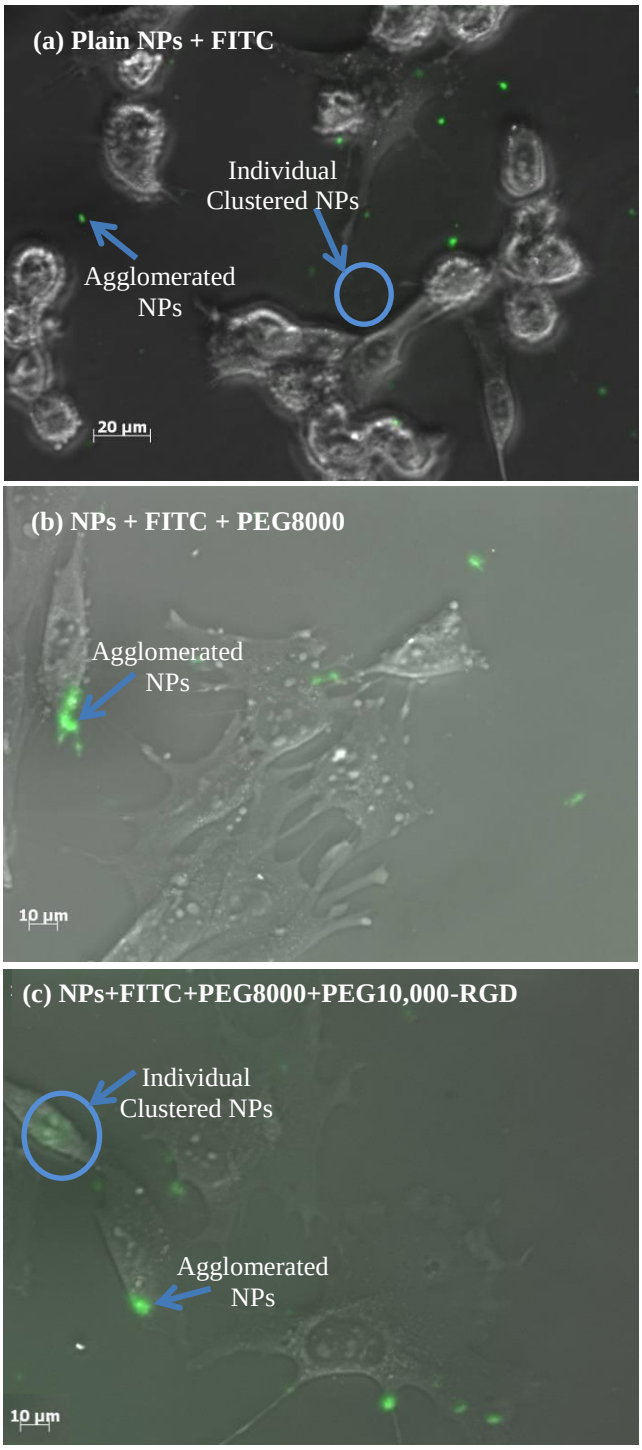

Figure 4.9. Merged phase contrast and fluorescent microscopy images of C17.2s with (a) Plain NPs + FITC, (b) NPs + FITC + PEG8000, (c) NPs + FITC + PEG8000 + PEG10,000-RGD.

Conclusion

In this study, I successfully synthesized silica nanoparticles, with and without PEG modifications. These materials were characterized using transmission electron microscopy, fourier transform infrared spectroscopy, and thermogravimentric analysis. Results from initial cell studies were positive; cells survived short-term incubation with all three populations of nanoparticles: (a) Plain NPs + FITC, (b) NPs + FITC + PEG8000, and (c) NPs + FITC + PEG8000 + PEG10,000-RGD.

The application of this work is to investigate ligand-receptor binding. Little is currently known about the way nanomaterials interact with cellular receptors. The affinities with which integrins bind with their ligands are often dependent upon force [90, 122-125]. The binding interaction between the receptor and targeting ligand should induce downstream signaling effects, though it is unclear how the mechanics of the ligand-binding event are implicated [89, 90]. PEGylated SiO_2 NPs with and without peptide conjugation are synthesized to investigate the mechanics of binding events between ligand-modified NPs and integrin. The RGD peptide, from fibronectin type III, is implicated both in cell adhesion through integrin $\alpha 5\beta 1$ as well as talin binding and mechanotransduction through integrin $\alpha v\beta 3$ [126, 127]. The compressive modulus of the PEG will modulate the mechanical environment of the cells, and the peptide modification will couple this mechanical signaling to a biochemical receptor-ligand binding event, effectively modulating chemical and mechanical signaling in a single platform. This combinatorial platform will allow for future observation and quantification of NP-integrin binding.

Before it can be used to investigate ligand binding, this PEGylated, RGD-functionalized NP platform will need to be further characterized. Particle size will be further examined using Dynamic Light Scattering (DLS) and TEM. Surface chemistry and peptide binding will be examined with X-ray Photoelectron Spectroscopy (XPS) with peptides containing iodo-tyrosine and UV-Vis Spectroscopy. Particle surface morphology will be investigated using Atomic force microscopy (AFM) and mechanical characterization of the NP-PEG complexes will be performed using AFM-enabled nanoindentation. Following material and mechanical profiling, biological activity of the NPs will be demonstrated using modified ELISA techniques and competitive binding assays, as well as further investigation of NP-cell interactions using confocal microscopy.

This work provides a foundation in the development of a nanoparticle-based chemo-mechanical system to investigate cell differentiation. Following further material and biological characterization, this will serve as a valuable nanoscale tool to induce and investigate ligand-receptor binding based cell behaviors. The platform provides versatility through tunability of PEG compressive modulus and peptide functionalization, which can be tailored to cell type and application.

Acknowledgements

The research was supported by NSF CBET #1014957. Additional thanks to Dr. Evan Snyder, of the Sanford-Burnham Medical Research Institute, for providing the C17.2 neural stem cells. Thanks to Dr. Masashi Watanabe and C. Austin Wade for their

assistance with TEM and Dr. Mark Snyder for his expertise in silica nanoparticle synthesis.

Chapter 5

Proteomic Analysis of C17.2 Neural Stem Cells Throughout Differentiation

Introduction

Neuronal differentiation consists of several morphological and biochemical landmarks including neuronal migration, axon outgrowth, and synapse formation [128, 129]. These processes are accompanied by cellular secretions and are regulated by molecules such as neurotrophins and insulin-like growth factors which surround the cells in the developing neural environment [130]. Analysis of these secreted molecules will provide to further understanding of neuronal development to improve therapeutics for nervous system developmental disorders and neurodegenerative disease.

Secreted proteins from cells make up a rich, complex population of molecules referred to as the secretome. Secreted proteins constitute an important class of molecules, which are encoded by approximately 10% of the human genome [131]. In recent years, several studies have been reported on stem cell secretome that have identified molecules active in physiological and pathological processes [132-134]. In addition, secretome profiling of primary cells isolated from a variety of tissues and species has become an active area of research [95-97]. Typical secreted proteins include serum proteins (*e.g.* albumin, transferrin immunoglobulins), extracellular matrix proteins (e.g. collagens, proteoglycans, fibronectin, laminins), digestive enzymes (e.g. trypsin) or milk proteins, though molecular detection depends greatly upon cell type. Secreted molecules that are more specific to cell type tend to be lower in abundance, though highly bioactive. This

category includes growth factors, hormones, cytokines and extracellular matrix-processing proteases, which have all been seen to play a key role in the regulation of cell renewal and differentiation [135].

Understanding the role of the secreted factors that direct and mark differentiation of these C17.2 NSCs *in vitro* is a fundamental prerequisite for suitable for therapeutic applications. This profiling, in addition to previously discussed biomaterial experiments, expands the characterization of the C17.2 cell line and extends its application as a relevant cell model. This work examines the C17.2 secretome throughout the 21 day differentiation period in order to identify unique proteins secreted at particular time points for use as biomarkers. Similar characterizations have been performed for other differentiating cell types, such as myoblasts and enterocytes [95-97].

In the neural environment, secreted proteins can act as chemoattractants or chemorepellants, which play a large role in neuronal migration and development [98]. These secreted molecules, in combination with the extracellular environment, can impact neuronal differentiation [99, 100]. Deducing the dynamics of neuronal cell secretions and developing a differentiation timeline will have a major impact on neuronal biology, translational therapeutics, and pharmaceutical research.

Figure 5.1 outlines the proteomics workflow to identify potential biomarkers of differentiation. This work presents a method of two dimensional gel electrophoresis with a bottom-up proteomics approach to determine which proteins are expressed at what time points as cells differentiate. Two dimensional gel electrophoresis separates proteins by isoelectric point and mass. Proteins are more effectively separated in 2D electrophoresis than 1D because it is unlikely that two molecules will be similar in two distinct properties. This separation technique will allow for identification of differences in protein expression across time points. Proteomic techniques are then used to identify the proteins

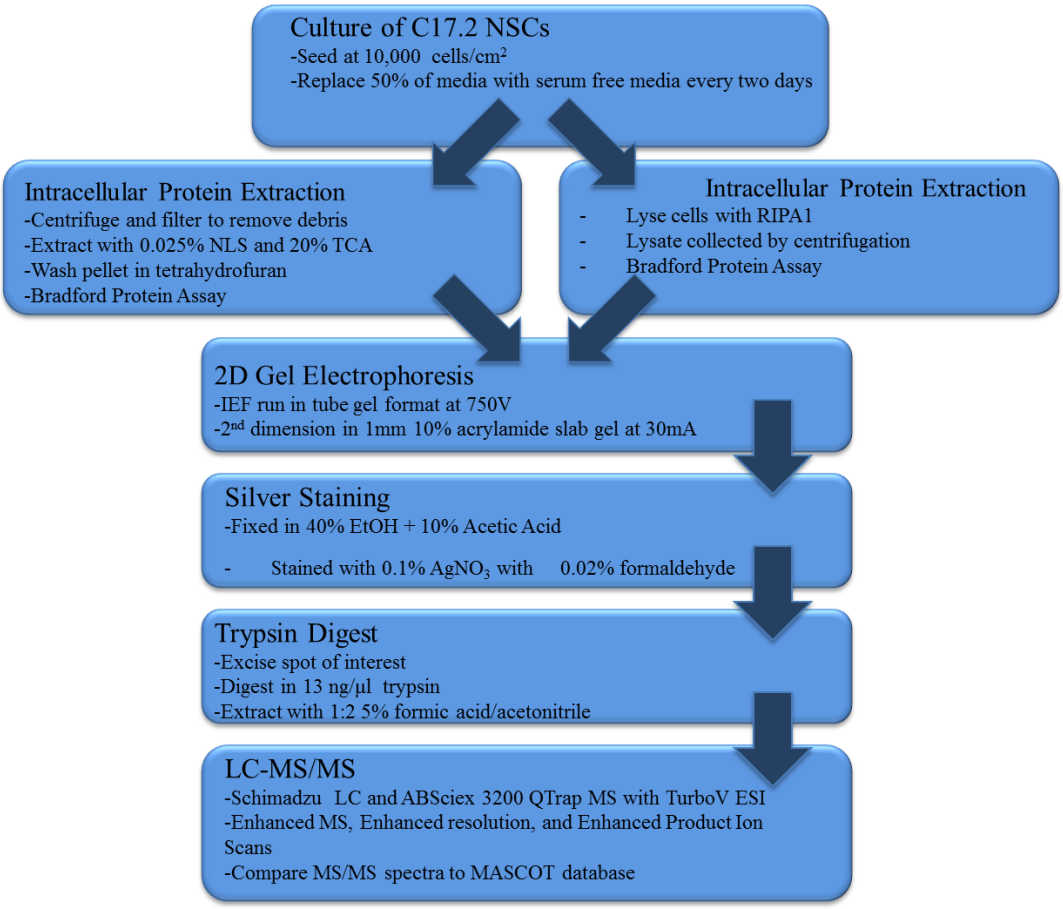

Figure 5.1. Workflow for proteomic characterization of C17.2 cells throughout differentiation.

of interest. In bottom-up proteomics, proteins are digested into peptide fragments prior to analysis by mass spectrometry. Proteins are then identified by cleavage products and MS/MS fragmentation. These products are then compared to the Swiss-Prot database to identify proteins of interest.

The work presented here is part of an interdisciplinary collaboration to develop a multi-functional platform to sense, decipher, and control cell fate. A tailored microfluidic culture environment will be coupled with nanoplasmonic sensing to detect cellular secretions in real time. A protein(s) of interest must be identified in order to further design the molecular sensor. By determining molecules of interest, the system can be customized to monitor these markers throughout differentiation.

Materials and Methods

Cell Culture: C17.2 neural stem cells, obtained from Dr. Evan Snyder at the Burnham Institute, were maintained in high-glucose DMEM containing 10% FBS, 5% horse serum, and 2mM L-Glutamine. Cells were passaged at 80-90% confluency using cell stripper. All experiments were performed with cells at passage number 20 or below. Cells were seeded onto three 10-cm polystyrene culture dishes at a density of 10,000 cells/cm^2 and allowed to grow to about 80% confluency, at which point the serum withdrawal process was started. Every 2 days, half of the media from each dish was removed and combined into 15 mL conical tube. 5mL serum-free culture media (DMEM high glucose with 1% L-Glutamine) was added to each dish to bring to keep the total media volume at 10mL.

Protein Extraction: Secreted proteins in collected cell media were extracted and concentrated for further analysis. Following removal from culture dish, media was

centrifuged at 1000xg for 5 minutes, filtered through a 0.2μm syringe filter, and cooled on ice. Anionic detergent N-lauroyl sarcosinate was added to 0.025% and mixed on ice for 5 minutes. 100% trichloroacetic acid was added to 20% to precipitate proteins in culture media. Samples were incubated on ice overnight to promote precipitation. Samples were then centrifuged at 4000xg and washed repeatedly with ice cold tetrahydrofuran, resuspending pellet between washes. Pellets were stored in a small volume of THF at -80°C.

Isoelectric Focusing: In order to identify proteins of interest within the C17.2 secretome, they were separated using 2D gel electrophoresis. The first step of this process is isoelectric focusing, which separates proteins based on isoelectric point. One end of a glass tube was sealed with parafilm. The casting tube was then filled with 1mm capillary tubes using glass rods to take up unused space as necessary. Prior to casting, the tube was immobilized in the vertical position using a clamp and ring stand. In order to make tube gels for the first dimension, an acrylamide solution was prepared (8.0 M urea, 4% acrylamide (total monomer), 2% Triton X-100, 1.6% Bio-Lyte 5/7 ampholyte, 0.4% Bio-Lyte 3/10 ampholyte, 0.1% TEMED) and degassed for 30 minutes. Following degassing, 10 µl of TEMED and 30 µl of 10% ammonium persulfate were added to induce polymerization. Gel solution was injected into the tube to cover the capillary tubes, taking care to not introduce bubbles, and allowed to polymerize for 1 hour. Following gel casting, the tubes were mounted and secured in the IEF apparatus. Upper Chamber Buffer (100mM NaOH) and Lower Chamber Buffer (10mM H_3PO_4) were prepared and degassed for 30 minutes. Protein pellets were solubilized in 6M urea and

mixed with IEF sample buffer (8.0 M urea, 2.0% Triton X-100, 10% Triton X-100, 5% β-mercaptoethanol, 1.6% Bio-Lyte 5/7 ampholyte, 0.4% Bio-Lyte 3/10 ampholyte). Samples were loaded into the sample chambers, carefully removing any bubbles that appeared, and topped with 20µL overlay buffer (4.0 M urea, 0.8% Bio-Lyte 5/7 ampholyte, 0.2% Bio-Lyte 3/10 ampholyte, 0.00005% Bromophenol blue). Samples were run at 750V until fully focused.

SDS-PAGE: Following isoelectric focusing, samples were run on an SDS-PAGE. A 1mm 10% acrylamide slab gel (4.5 ml of distilled water, 2ml of 2M Tris HCL, 3.3 ml of 30% acrylamide/Bis, 100 µl of 10% SDS, 8 µl TEMED, 30 µl 10% APS) was cast using the casting apparatus. The polymerizing gel was overlaid with water-saturated butanol to achieve a smooth gel surface. Following polymerization, the gel surface was thoroughly rinsed with dd$H_2$0 to remove butanol. The first dimension tube gels were ejected from the capillary tubes, position on top of the slab gel, and topped with SDS sample equilibration buffer (0.0625 M Tris HCl, pH 6.8, 2.3% SDS, 5.0% β-mercaptoethanol, 10% glycerol (w/v), 0.0005% bromophenol blue). The second dimension was run in 1X running buffer (25 mM Tris, 192 mM glycine, 0.1% SDS) at 45mA for 5 hours.

Silver Staining: Silver staining was selected as the method of visualization for the 2D gels due to its high sensitivity and compatibility with downstream mass spectrometry analysis. Staining was performed according to the methods of Mortz et al. 2001 [136]. Briefly, gels were fixed (40% ethanol, 10% acetic acid) for 1 hour, washed thoroughly in ddH_2O, sensitized in 0.02% sodium thiosulfate, rinsed again in ddH_2O, and incubated with cold silver stain (0.1% silver nitrate + 0.02% formaldehyde) for 20 minutes. Gels

were rinsed, transferred to a new tray, and developed in 3% sodium carbonate + 0.05% formaldehyde. Staining was terminated with 5% acetic acid for 5 minutes. Gels were stored at 4°C in 1% acetic acid.

Results and Discussion

Protein Extraction: Several sample sets have been collected. Samples after day, below 1% serum, as shown in Table 5.1, are of particular interest; above this point, albumin from the serum-containing media overwhelms the samples. Protein samples were extracted, washed in tetradhydrofuran, and pelleted for storage at -80°C. Sample aliquots are currently stored in the Jedlicka lab at -80°C.

	% Total Serum
Day 1	15.00%
Day 3	7.50%
Day 5	3.75%
Day 7	1.88%
Day 9	0.94%
Day 11	0.47%
Day 13	0.23%
Day 15	0.12%
Day 17	0.0586%
Day 19	0.0293%
Day 21	0.0146%

Table 5.1. Schedule of serum withdrawal for C17.2s. Data points below 1% are of particular interest due to the lower levels of albumin from serum-containing media.

Two Dimensional Gel Electrophoresis: A method was developed for two dimensional gel electrophoresis followed by mass spec compatible silver staining. Isoelectric focusing was performed using the Mini-PROTEAN 2-D tube module and electrophoresis cell (BioRad). Initial focusing was performed with a 300V power supply, which was insufficient for complete focusing, as seen in Figure 5.2a. A higher voltage power supply was purchased, PowerPac HV Power Supply (BioRad), and future focusing was performed at 750V. This addressed the issue of completeness of isoelectric focusing, as seen in Figure 5.2b. Furthermore, any slight bubble in the chamber buffers, tube gels, or samples will cause an interruption in the circuit and interrupt focusing.

Due to time constraints and limited supply of secretome samples, two dimensional gels were not performed for all timepoints. Collected samples will be stored at -80°C and sent to the Proteomics Core Facility in the Penn Genomics Institute at the University of Pennsylvania for further analysis and identification.

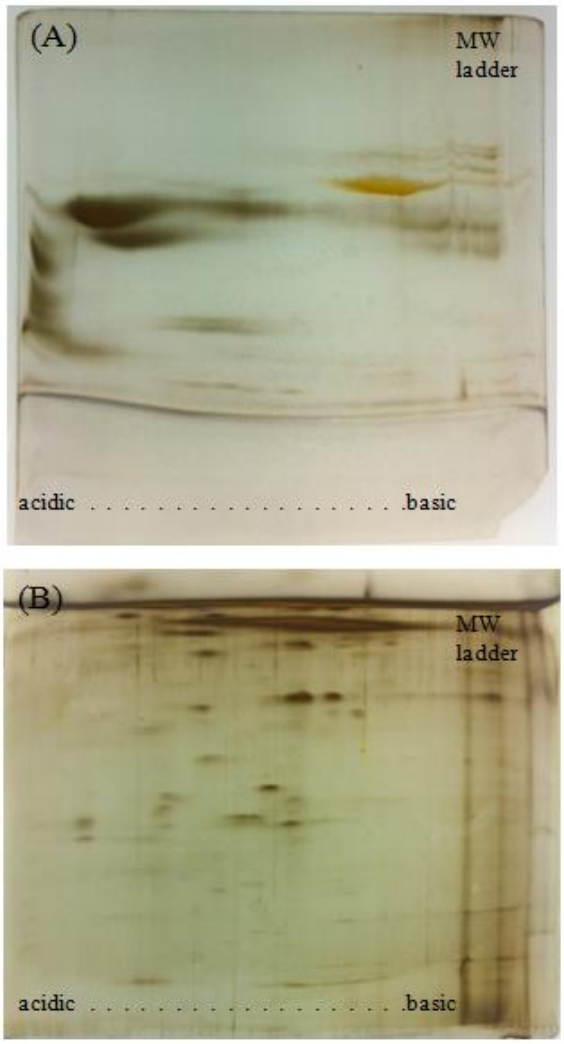

Figure 5.2. Representative two dimensional gels separated horizontally by isoelectric point and vertically by size. (A) shows incomplete separation due to incomplete isoelectric focusing. (B) shows more complete focusing.

Mass Spectrometry: I successfully completed a training course with ABSciex, titled "5500/4000 QTRAP System Peptide Quant Training", in preparation for use of the 3200 QTRAP instrument at Lehigh. In addition to classroom training, I was trained on the Lehigh instrument by Dr. Jesús Gonzalez. I optimized liquid chromatography solvents

and methods to optimize separation of trypsin digest products prior to mass spec analysis. I worked with a β-galactosidase standard (Protea) to learn about the different variables and controls within the mass spec instrument. Following separation by LC, the sample is introduced into ion source, ionized, focused into mass analyzer, detected and a signal sent to data system where m/z ratio is recorded with relative intensity. As the sample comes of the LC, the mass spec runs continuously, collecting intensity vs m/z ratio data for each time point. At this point, the fragments being detected are the fragments that were created by the trypsin digest. In general, peptides can be identified by fragmenting them in MS, as peptides fragment in characteristic ways. For every MS scan, the most intense peaks are selected and those ions are then selected for fractionation. The ions collide with gas within the instrument and the bonds within the peptides break in characteristic ways. The resulting fragment ions have mass differences corresponding to the residue masses of the respective amino acids. Figure 5.3 shows a data from a single time point. The top panel is the scan of all peptide species at that time point. The second panel identifies the peptides for fractionation, and the lower two panels are the products of fractionation. The data set, composed of MS/MS spectra from each time point, can then be compared to a database such as Swiss Prot to identify proteins in the sample. If one or more peptide sequences are unique to that protein, or a combination of enough peptides, you can confidently determine the identity of the protein.

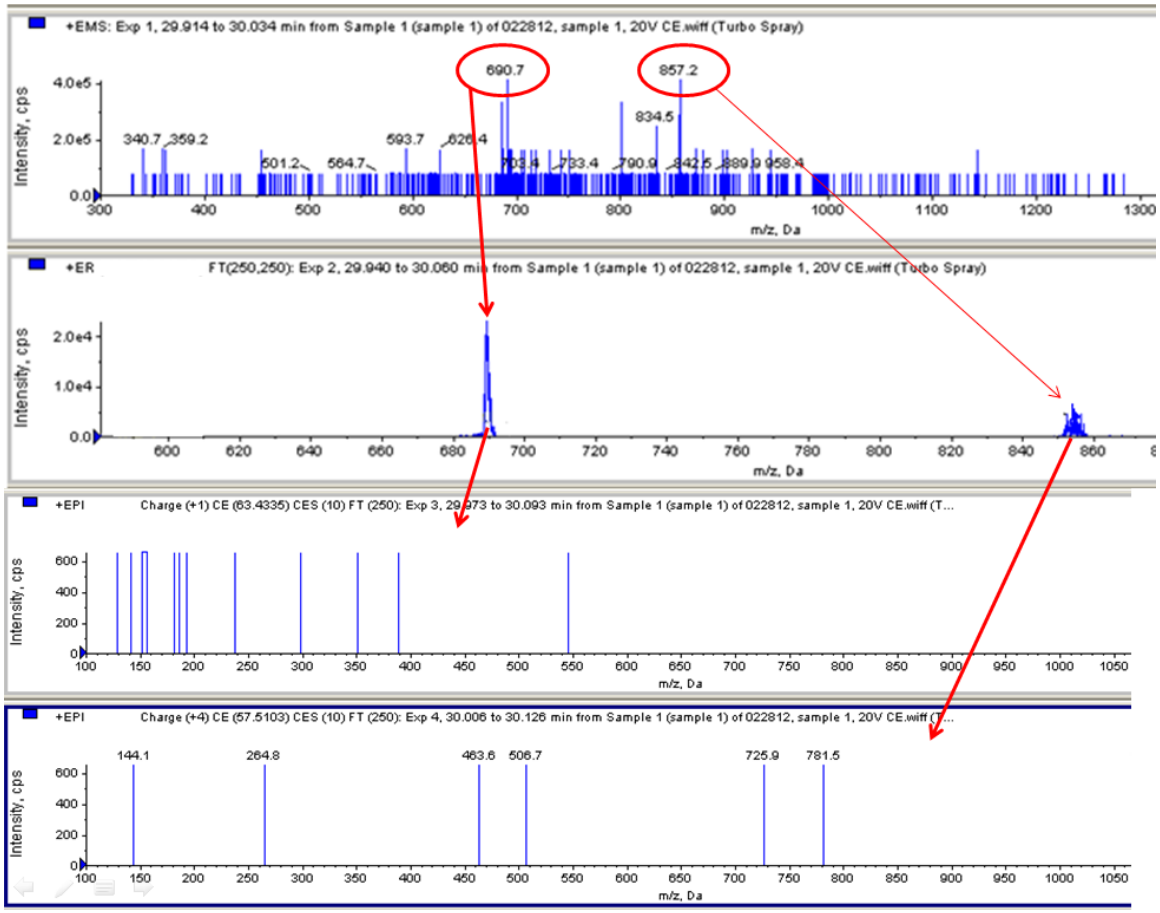

Figure 5.3. Representative LC-MS/MS data from a single time point for a β-galactosidase standard

Due to a costly instrument repair (interface heater malfunction), work on this study was suspended. As discussed previously, samples will be stored until they can be sent to the Proteomics Core Facility in the Penn Genomics Institute at the University of Pennsylvania for further analysis and identification.

Conclusion

The methods prevented above have been selected and troubleshot in order to characterize the secretome of C17.2 neurons throughout differentiaton. By identifying unique secreted molecules at particular timepoints, a molecular timeline of differentiation

can be developed. This information is incredibly valuable to the general study of NSC differentiation and, more specifically, to the development of a combined culture environment and molecular detector. Several sets of samples have been collected and are currently stored in the Jedlicka lab at -80°C. Samples will be sent to the Proteomics Core Facility in the Penn Genomics Institute at the University of Pennsylvania for further analysis and identification. There, the samples will be subjected to a similar 2D gel electrophoresis and mass spectrometry protocol to the one outlined here. Resulting spectra will then be analyzed. Proteins will be identified by comparison to the *Mus musculus* entries of the Swiss-Prot database. Fixed modification, mass tolerance of 50 ppm, carbamidomethylation of cysteines, and oxidation of methionine will all be considered in the identification process. Additional parameters will be set as necessary. The compounds identified in the secretome analysis will provide potential molecules to examine to map the secretome during the course of neuronal differentiation.

Chapter 6

Conclusion

In this study, I have provided valuable characterization of material substrates used to investigate the effects of chemo-mechanical factors on neural stem cell differentiation. In Chapter 2, substrate stiffness was verified, and found to support values published by Yeung et al. [1]. A method for quantifying bound collagen was developed, and preliminary cell studies confirm the hypothesis that softer substrates would support neuronal differentiation better than stiffer substrates. Additional experiments, in combination with collagen quantification, would allow for statistical analysis to determine if and how collagen density impacts C17.2 differentiation in combination with substrate stiffness. Chapter 3 provides the framework to expand the polyacrylamide-collagen system to a more controllable and more easily tunable peptide-based system. Future work in both of these substrate platforms includes a continuation of work performed by Colleen Curley. In addition to neurite measurements, specimens will be assessed for formation of synapses. Colleen observed synaptogenesis in C17.2s cultured on polyacrylamide gels, but this has not yet been characterized across various collagen concentrations. Finally, further analysis of neuronal subtypes, through additional immunocytochemical staining and PCR, will provide insight to the functionality of the mature neurons produced. Results from this work further the knowledge base for the design of biomaterials scaffold to direct neural stem cell fate, with applications in cellular implants for treatment of neurodegenerative diseases.

PEGylated nanoparticles were designed and synthesized to investigate ligand-receptor binding and its effect on downstream signaling. Initial characterization results were positive: the presence of PEG was confirmed through FTIR and TGA and cells survived short-term exposure to nanoparticles. Peptide binding will need to be verified with X-ray Photoelectron Spectroscopy (XPS) and UV-Vis Spectroscopy. With further characterization, including particle size by DLS and TEM, surface morphology by AFM, mechanical compressibility by AFM-enabled nanoindentation, and biological activity by modified ELISA techniques and competitive binding assays, this combinatorial platform will be a valuable tool for observation and quantification of NP-integrin binding.

Finally, Chapter 5 presents a framework to investigate the secretome of differentiating C17.2s. Through knowledge of unique secretions throughout this process, a molecular timeline can be constructed. This information is incredibly valuable to the general study of NSC differentiation and, more specifically, to the development of a combined culture environment and molecular detector. Due to time constraints and equipment limitations, samples will be sent to the Proteomics Core Facility in the Penn Genomics Institute at the University of Pennsylvania for further analysis and identification. This timeline of differentiation, in combination with the chemo-mechanical substrate experiments, will greatly contribute to the characterization of the C17.2 cell line and improve its relevance as a neural stem cell model.

List of References

1. Yeung, T., Georges, P. C., Flanagan, L. A., Marg, B., Ortiz, M., Funaki, M., Zahir, N., Ming, W., Weaver, V., & Janmey, P. A. "Effects of substrate stiffness on cell morphology, cytoskeletal structure, and adhesion." *Cell motility and the cytoskeleton* 60.1 (2005): 24-34.
2. Engler, A. J., Griffin, M. A., Sen, S., Bönnemann, C. G., Sweeney, H. L., & Discher, D. E. "Myotubes differentiate optimally on substrates with tissue-like stiffness pathological implications for soft or stiff microenvironments."*The Journal of cell biology* 166.6 (2004): 877-887.
3. Engler, A. J., Sen, S., Sweeney, H. L., & Discher, D. E. "Matrix elasticity directs stem cell lineage specification." *Cell* 126.4 (2006): 677-689.
4. Guilak, F., Cohen, D. M., Estes, B. T., Gimble, J. M., Liedtke, W., & Chen, C. S. "Control of stem cell fate by physical interactions with the extracellular matrix." *Cell stem cell* 5.1 (2009): 17-26.
5. Rosser, A. E., Zietlow, R., & Dunnett, S. B. . "Stem cell transplantation for neurodegenerative diseases." *Current opinion in neurology*20.6 (2007): 688-692.
6. Callister, William D., and David G. Rethwisch. *Fundamentals of materials science and engineering: an integrated approach*. Wiley. com, 2012.
7. Pelham, R. J., & Wang, Y. L. "Cell locomotion and focal adhesions are regulated by substrate flexibility." *Proceedings of the National Academy of Sciences* 94.25 (1997): 13661-13665.
8. Engler, A., Bacakova, L., Newman, C., Hategan, A., Griffin, M., & Discher, D. "Substrate compliance versus ligand density in cell on gel responses." *Biophysical journal* 86.1 (2004): 617-628.
9. Solon, J., Levental, I., Sengupta, K., Georges, P. C., & Janmey, P. A."Fibroblast adaptation and stiffness matching to soft elastic substrates." *Biophysical journal* 93.12 (2007): 4453-4461.
10. Flanagan, L. A., Ju, Y. E., Marg, B., Osterfield, M., & Janmey, P. A. "Neurite branching on deformable substrates."*Neuroreport* 13.18 (2002): 2411.
11. Discher, D. E., Janmey, P., & Wang, Y. L. "Tissue cells feel and respond to the stiffness of their substrate." *Science* 310.5751 (2005): 1139-1143.
12. Paszek, M. J., Zahir, N., Johnson, K. R., Lakins, J. N., Rozenberg, G. I., Gefen, A., Reinhart-King, C.A., Marguiles, S.S., Dembo, M., Boettiger, D., Hammer, D.A., & Weaver, V. M. "Tensional homeostasis and the malignant phenotype." *Cancer cell* 8.3 (2005): 241-254.
13. Kloxin, A. M., Benton, J. A., & Anseth, K. S. "In situ elasticity modulation with dynamic substrates to direct cell phenotype."*Biomaterials* 31.1 (2010): 1-8.
14. Genes, N. G., Rowley, J. A., Mooney, D. J., & Bonassar, L. J. "Effect of substrate mechanics on chondrocyte adhesion to modified alginate surfaces." *Archives of biochemistry and biophysics* 422.2 (2004): 161-167.

15. Balgude, A. P., Yu, X., Szymanski, A., & Bellamkonda, R. V. "Agarose gel stiffness determines rate of DRG neurite extension in 3D cultures." *Biomaterials* 22.10 (2001): 1077-1084.
16. Harris, A. K., Wild, P., & Stopak, D.. "Silicone rubber substrata: a new wrinkle in the study of cell locomotion." *Science* 208.4440 (1980): 177-179.
17. Brown, X. Q., Ookawa, K., & Wong, J. Y. "Evaluation of polydimethylsiloxane scaffolds with physiologically-relevant elastic moduli: interplay of substrate mechanics and surface chemistry effects on vascular smooth muscle cell response." *Biomaterials* 26.16 (2005): 3123-3129.
18. Martinac, B. "Mechanosensitive ion channels: molecules of mechanotransduction." *Journal of cell science* 117.12 (2004): 2449-2460.
19. Gao, M., Craig, D., Vogel, V., & Schulten, K. "Identifying Unfolding Intermediates of FN-III(1) by Steered Molecular Dynamics." *Journal of molecular biology* 323.5 (2002): 939-950.
20. Hsu, H. J., Lee, C. F., Locke, A., Vanderzyl, S. Q., & Kaunas, R. "Stretch-induced stress fiber remodeling and the activations of JNK and ERK depend on mechanical strain rate, but not FAK." *PLoS One*5.8 (2010): e12470.
21. Vogel, V. & Sheetz, M. "Local force and geometry sensing regulate cell functions." *Nature Reviews Molecular Cell Biology* 7.4 (2006): 265-275.
22. Orr, A. W., Helmke, B. P., Blackman, B. R., & Schwartz, M. A. "Mechanisms of mechanotransduction." *Developmental cell* 10.1 (2006): 11-20.
23. Janmey, P. A., & Weitz, D. A. "Dealing with mechanics: mechanisms of force transduction in cells." *Trends in biochemical sciences* 29.7 (2004): 364-370.
24. Geiger, B. & Bershadsky, A. "Exploring the neighborhood: adhesion-coupled cell mechanosensors." *Cell* 110.2 (2002): 139-142.
25. Ingber, D.E. "Cellular mechanotransduction: putting all the pieces together again." *The FASEB Journal* 20.7 (2006): 811-827.
26. Quinlan, A. M. T., Sierad, L. N., Capulli, A. K., Firstenberg, L. E., & Billiar, K. L. "Combining dynamic stretch and tunable stiffness to probe cell mechanobiology in vitro." *PloS one* 6.8 (2011): e23272.
27. Burridge, K., & Chrzanowska-Wodnicka, M. "Focal adhesions, contractility, and signaling." *Annual review of cell and developmental biology*12.1 (1996): 463-519.
28. Juliano, R. L., & Haskill, S. "Signal transduction from the extracellular matrix." *Journal of Cell Biology* 120 (1993): 577-577.
29. Craig, S. W., & Johnson, R. P. "Assembly of focal adhesions: progress, paradigms, and portents." *Current opinion in cell biology* 8.1 (1996): 74-85.
30. Chrzanowska-Wodnicka, M., & Burridge, K. "Rho-stimulated contractility drives the formation of stress fibers and focal adhesions." *The Journal of cell biology* 133.6 (1996): 1403-1415.
31. Banes, A. J., Tsuzaki, M., Yamamoto, J., Brigman, B., Fischer, T., Brown, T., & Miller, L. "Mechanoreception at the cellular level: the detection, interpretation, and diversity of responses to mechanical signals." *Biochemistry and Cell Biology* 73.7-8 (1995): 349-365.
32. Robling, A. G., Castillo, A. B., & Turner, C. H. "Biomechanical and molecular regulation of bone remodeling." *Annu. Rev. Biomed. Eng.* 8 (2006): 455-498.

33. Feng, Y., & Walsh, C. A. "Protein–protein interactions, cytoskeletal regulation and neuronal migration." *Nature Reviews Neuroscience*2.6 (2001): 408-416.
34. Dent, E. W., & Gertler, F. B. "Cytoskeletal dynamics and transport in growth cone motility and axon guidance." *Neuron* 40.2 (2003): 209-227.
35. Dickson, B. J. "Molecular mechanisms of axon guidance." *Science*298.5600 (2002): 1959-1964.
36. Dent, E. W., Tang, F., & Kalil, K. "Axon guidance by growth cones and branches: common cytoskeletal and signaling mechanisms." *The Neuroscientist* 9.5 (2003): 343-353.
37. Tang, Y., Shah, K., Messerli, S. M., Snyder, E., Breakefield, X., & Weissleder, R. "In vivo tracking of neural progenitor cell migration to glioblastomas." *Human gene therapy* 14.13 (2003): 1247-1254.
38. Robles, E., & Gomez, T. M. "Focal adhesion kinase signaling at sites of integrin-mediated adhesion controls axon pathfinding." *Nature neuroscience* 9.10 (2006): 1274-1283.
39. Anderson, H., and Tucker, R.P. "Pioneer neurones use basal lamina as a substratum for outgrowth in the embryonic grasshopper limb." *Development* 104.4 (1988): 601-608.
40. Scherer, S. S., & Easter Jr, S. S. "Degenerative and regenerative changes in the trochlear nerve of goldfish." *Journal of neurocytology* 13.4 (1984): 519-565.
41. Chou, S. Y., Cheng, C. M., Chen, C. C., & LeDuc, P. R. "Localized neurite outgrowth sensing via substrates with alternative rigidities." *Soft Matter* 7.21 (2011): 9871-9877.
42. Keung, A. J., de Juan-Pardo, E. M., Schaffer, D. V., & Kumar, S. "Rho GTPases mediate the mechanosensitive lineage commitment of neural stem cells." *Stem Cells* 29.11 (2011): 1886-1897.
43. Saha, K., Keung, A. J., Irwin, E. F., Li, Y., Little, L., Schaffer, D. V., & Healy, K. E. "Substrate modulus directs neural stem cell behavior."*Biophysical journal* 95.9 (2008): 4426-4438.
44. Keung, A. J., Dong, M., Schaffer, D. V., & Kumar, S. "Pan-neuronal maturation but not neuronal subtype differentiation of adult neural stem cells is mechanosensitive." *Scientific reports*3 (2013).
45. Takahashi, J., Palmer, T. D., & Gage, F. H. "Retinoic acid and neurotrophins collaborate to regulate neurogenesis in adult-derived neural stem cell cultures." *Journal of neurobiology* 38.1 (1999): 65-81.
46. Curley, C. T., Fanale, K., & Jedlicka, S. S. "Characterizing the effect of substrate stiffness on neural stem cell differentiation." *MRS Online Proceedings Library* 1498.1 (2012).
47. Frantz, C., Stewart, K. M., & Weaver, V. M. "The extracellular matrix at a glance." *Journal of Cell Science* 123.24 (2010): 4195-4200.
48. Clark, E. A., & Brugge, J. S. "Integrins and signal transduction pathways: the road taken." *Science* 268.5208 (1995): 233-239.
49. Schlaepfer, D. D., Hanks, S. K., Hunter, T., & van der Geer, P. "Integrin-mediated signal transduction linked to Ras pathway by GRB2 binding to focal adhesion kinase." (1994): 786-791.

50. Jalali, S., del Pozo, M. A., Chen, K. D., Miao, H., Li, Y. S., Schwartz, M. A., Shyy, J.Y.J., & Chien, S. "Integrin-mediated mechanotransduction requires its dynamic interaction with specific extracellular matrix (ECM) ligands." *Proceedings of the National Academy of Sciences* 98.3 (2001): 1042-1046.
51. Giancotti, F. G., & Ruoslahti, E. "Integrin signaling." *Science*285.5430 (1999): 1028-1033.
52. Werb, Z., Tremble, P. M., Behrendtsen, O., Crowley, E., & Damsky, C. H. "Signal transduction through the fibronectin receptor induces collagenase and stromelysin gene expression." *The Journal of Cell Biology*109.2 (1989): 877-889.
53. Hall, D. E., Reichardt, L. F., Crowley, E., Holley, B., Moezzi, H., Sonnenberg, A., & Damsky, C. H. "The alpha 1/beta 1 and alpha 6/beta 1 integrin heterodimers mediate cell attachment to distinct sites on laminin." *The Journal of cell biology*110.6 (1990): 2175-2184.
54. Pierschbacher, M. D., & Ruoslahti, E. "Cell attachment activity of fibronectin can be duplicated by small synthetic fragments of the molecule."*Nature* 309.5963 (1983): 30-33.
55. D'Souza, S. E., Ginsberg, M. H., Burke, T. A., Lam, S. C., & Plow, E. F. "Localization of an Arg-Gly-Asp recognition site within an integrin adhesion receptor." *Science* 242.4875 (1988): 91-93.
56. Plopper, G. E., McNamee, H. P., Dike, L. E., Bojanowski, K., & Ingber, D. E. "Convergence of integrin and growth factor receptor signaling pathways within the focal adhesion complex." *Molecular Biology of the Cell* 6.10 (1995): 1349.
57. Burridge, K., Fath, K., Kelly, T., Nuckolls, G., & Turner, C. "Focal adhesions: transmembrane junctions between the extracellular matrix and the cytoskeleton." *Annual review of cell biology* 4.1 (1988): 487-525.
58. Kubota, Y., Kleinman, H. K., Martin, G. R., & Lawley, T. J. "Role of laminin and basement membrane in the morphological differentiation of human endothelial cells into capillary-like structures." *The Journal of Cell Biology* 107.4 (1988): 1589-1598.
59. Rogers, S. L., Letourneau, P. C., Palm, S. L., McCarthy, J., & Furcht, L. T. . "Neurite extension by peripheral and central nervous system neurons in response to substratum-bound fibronectin and laminin."*Developmental biology* 98.1 (1983): 212-220.
60. Sternberg, J., & Kimber, S. J. "Distribution of fibronectin, laminin and entactin in the environment of migrating neural crest cells in early mouse embryos."*Journal of embryology and experimental morphology* 91.1 (1986): 267-282.
61. Duband, J. L., & Thiery, J.P. "Distribution of laminin and collagens during avian neural crest development." *Development* 101.3 (1987): 461-478.
62. Duband, J. L., Rocher, S., Chen, W. T., Yamada, K. M., & Thiery, J. P. "Cell adhesion and migration in the early vertebrate embryo: location and possible role of the putative fibronectin receptor complex."*The Journal of cell biology* 102.1 (1986): 160-178.

63. Krotoski, D. M., Domingo, C., & Bronner-Fraser, M. "Distribution of a putative cell surface receptor for fibronectin and laminin in the avian embryo." *The Journal of cell biology* 103.3 (1986): 1061-1071.
64. Evercooren, B. V., Kleinman, H. K., Ohno, S., Marangos, P., Schwartz, J. P., & Dubois-Dalcq, M. E.. "Nerve growth factor, laminin, and fibronectin promote neurite growth in human fetal sensory ganglia cultures." *Journal of neuroscience research* 8.2-3 (1982): 179-193.
65. Lander, A. D., Fujii, D. K., & Reichardt, L. F. . "Laminin is associated with the" neurite outgrowth-promoting factors" found in conditioned media." *Proceedings of the National Academy of Sciences* 82.7 (1985): 2183-2187.
66. Manthorpe, M., Engvall, E., Ruoslahti, E., Longo, F. M., Davis, G. E., & Varon, S. . "Laminin promotes neuritic regeneration from cultured peripheral and central neurons." *The Journal of cell biology* 97.6 (1983): 1882-1890.
67. Wewer, U., Albrechtsen, R., Manthorpe, M., Varon, S., Engvall, E., & Ruoslahti, E. "Human laminin isolated in a nearly intact, biologically active form from placenta by limited proteolysis." *Journal of Biological Chemistry*258.20 (1983): 12654-12660.
68. Edgar, D., Timpl, R., & Thoenen, H. "The heparin-binding domain of laminin is responsible for its effects on neurite outgrowth and neuronal survival."*The EMBO journal* 3.7 (1984): 1463.
69. Faivre-Bauman, A., Puymirat, J., Loudes, C., Barret, A., & Tixier-Vidal, A. "Laminin promotes attachment and neurite elongation of fetal hypothalamic neurons grown in serum-free medium." *Neuroscience letters* 44.1 (1984): 83-89.
70. Liesi, P., Dahl, D., & Vaheri, A. "Neurons cultured from developing rat brain attach and spread preferentially to laminin." *Journal of neuroscience research*11.3 (1984): 241-251.
71. Smalheiser, N. R., Crain, S. M., & Reid, L. M. "Laminin as a substrate for retinal axons in vitro." *Developmental Brain Research* 12.1 (1984): 136-140.
72. Adler, R., Jerdan, J., & Hewitt, A. T. "Responses of cultured neural retinal cells to substratum-bound laminin and other extracellular matrix molecules." *Developmental biology* 112.1 (1985): 100-114.
73. Hammarback, J. A., Palm, S. L., Furcht, L. T., & Letourneau, P. C. "Guidance of neurite outgrowth by pathways of substratum-adsorbed laminin." *Journal of neuroscience research* 13.1-2 (1985): 213-220.
74. Hammarback, J. A., & Letourneau, P. C. "Neurite extension across regions of low cell-substratum adhesivity: implications for the guidepost hypothesis of axonal pathfinding." *Developmental biology* 117.2 (1986): 655-662.
75. Hopkins, J. M., Ford-Holevinski, T. S., McCoy, J. P., & Agranoff, B. W. "Laminin and optic nerve regeneration in the goldfish." *The Journal of neuroscience* 5.11 (1985): 3030-3038.
76. Davis, G. E., Manthorpe, M., & Varon, S. "Parameters of neuritic growth from ciliary ganglion neurons in vitro: influence of laminin, schwannoma polyornithine-binding neurite promoting factor ciliary neuronotrophic factor."*Developmental Brain Research* 17.1 (1985): 75-84.

77. Engvall, E., Davis, G. E., Dickerson, K., Ruoslahti, E., Varon, S., & Manthorpe, M. "Mapping of domains in human laminin using monoclonal antibodies: localization of the neurite-promoting site." *The Journal of cell biology* 103.6 (1986): 2457-2465.
78. Hui, T. Y., Cheung, K. M. C., Cheung, W. L., Chan, D., & Chan, B. P. "In vitro chondrogenic differentiation of human mesenchymal stem cells in collagen microspheres: influence of cell seeding density and collagen concentration." *Biomaterials* 29.22 (2008): 3201-3212.
79. Nöth, U., Rackwitz, L., Heymer, A., Weber, M., Baumann, B., Steinert, A., Schütze, N., Jakob, F., & Eulert, J. . "Chondrogenic differentiation of human mesenchymal stem cells in collagen type I hydrogels." *Journal of Biomedical Materials Research Part A* 83.3 (2007): 626-635.
80. Ma, W., Fitzgerald, W., Liu, Q. Y., O'shaughnessy, T. J., Maric, D., Lin, H. J Alkon, D.L. & Barker, J. L. "CNS stem and progenitor cell differentiation into functional neuronal circuits in three-dimensional collagen gels." *Experimental neurology*190.2 (2004): 276-288.
81. Condic, M. L., & Letourneau, P. C. "Ligand-induced changes in integrin expression regulate neuronal adhesion and neurite outgrowth." *Nature*389.6653 (1997): 852-856.
82. Baugh, L., & Vogel, V. "Structural changes of fibronectin adsorbed to model surfaces probed by fluorescence resonance energy transfer." *Journal of Biomedical Materials Research Part A* 69.3 (2004): 525-534.
83. Antia, M., Islas, L. D., Boness, D. A., Baneyx, G., & Vogel, V. "Single molecule fluorescence studies of surface-adsorbed fibronectin." *Biomaterials* 27.5 (2006): 679-690.
84. Jedlicka, S. S., McKenzie, J. L., Leavesley, S. J., Little, K. M., Webster, T. J., Robinson, J. P., Nivens, D.E., & Rickus, J. L. "Sol-gel derived materials as substrates for neuronal differentiation: effects of surface features and protein conformation."*Journal of Materials Chemistry* 16.31 (2006): 3221-3230.
85. Jedlicka, S. S., Dadarlat, M., Hassell, T., Lin, Y., Young, A., Zhang, M., Irazoqui, P., & Rickus, J. L. "Calibration of neurotransmitter release from neural cells for therapeutic implants." *International journal of neural systems* 19.03 (2009): 197-212.
86. Jones-Villeneuve, E. M., McBurney, M. W., Rogers, K. A., & Kalnins, V. I "Retinoic acid induces embryonal carcinoma cells to differentiate into neurons and glial cells." *The Journal of cell biology*94.2 (1982): 253-262.
87. Dembo, M., & Wang, Y. L. "Stresses at the cell-to-substrate interface during locomotion of fibroblasts." *Biophysical journal* 76.4 (1999): 2307-2316.
88. Jedlicka, S. S., Little, K. M., Nivens, D. E., Zemlyanov, D., & Rickus, J. L. "Peptide ormosils as cellular substrates." *Journal of Materials Chemistry* 17.48 (2007): 5058-5067.
89. Bhattacharyya, S., Bhattacharya, R., Curley, S., McNiven, M. A., & Mukherjee, P. "Nanoconjugation modulates the trafficking and mechanism of antibody induced receptor endocytosis." *Proceedings of the National Academy of Sciences* 107.33 (2010): 14541-14546.

90. Basu, S., Chaudhuri, P., & Sengupta, S. "Targeting oncogenic signaling pathways by exploiting nanotechnology." *Cell Cycle* 8.21 (2009): 3480-3487.
91. Cauda, V., Argyo, C., & Bein, T. "Impact of different PEGylation patterns on the long-term bio-stability of colloidal mesoporous silica nanoparticles." *Journal of Materials Chemistry* 20.39 (2010): 8693-8699.
92. Snyder, E. Y., Deitcher, D. L., Walsh, C., Arnold-Aldea, S., Hartwieg, E. A., & Cepko, C. L.. "Multipotent neural cell lines can engraft and participate in development of mouse cerebellum." *Cell* 68.1 (1992): 33-51.
93. Flax, J. D., Aurora, S., Yang, C., Simonin, C., Wills, A. M., Billinghurst, L. L., Jendoubi, M., Sidman, R., Wolfe, J., Kim, S.U., Snyder, E. Y. "Engraftable human neural stem cells respond to development cues, replace neurons, and express foreign genes." *Nature biotechnology* 16.11 (1998): 1033-1039.
94. Boockvar, J. A., Schouten, J., Royo, N., Millard, M., Spangler, Z., Castelbuono, D., Snyder, E., O'Rourke, D., & McIntosh, T. "Experimental traumatic brain injury modulates the survival, migration, and terminal phenotype of transplanted epidermal growth factor receptor-activated neural stem cells." *Neurosurgery* 56.1 (2005): 163-171.
95. Le Bihan, M. C., Bigot, A., Jensen, S. S., Dennis, J., Rogowska-Wrzesinska, A., Lainé, J., Gache, V., Furling, D., Jensen, O.N., Voit, T., Mouly, V., Coutton, G.R., & Butler-Browne, G. "In-depth analysis of the secretome identifies three major independent secretory pathways in differentiating human myoblasts." *Journal of proteomics* (2012).
96. Henningsen, J., Rigbolt, K. T., Blagoev, B., Pedersen, B. K., & Kratchmarova, I. "Dynamics of the skeletal muscle secretome during myoblast differentiation." *Molecular & Cellular Proteomics* 9.11 (2010): 2482-2496.
97. García-Lorenzo, A., Rodríguez-Piñeiro, A. M., Rodríguez-Berrocal, F. J., Cadena, M. P. D. L., & Martínez-Zorzano, V. S. "Changes on the Caco-2 Secretome through Differentiation Analyzed by 2-D Differential In-Gel Electrophoresis (DIGE)."*International journal of molecular sciences* 13.11 (2012): 14401-14420.
98. Cayre, M., Canoll, P., & Goldman, J. E. "Cell migration in the normal and pathological postnatal mammalian brain." *Progress in neurobiology*88.1 (2009): 41-63.
99. Schubert, D. "Protein secretion by clonal glial and neuronal cell lines."*Brain research* 56 (1973): 387-391.
100. Schubert, D., Herrera, F., Cumming, R., Read, J., Low, W., Maher, P., & Fischer, W. H. "Neural cells secrete a unique repertoire of proteins."*Journal of neurochemistry* 109.2 (2009): 427-435.
101. Watt, F. M., & Hogan, B. L. "Out of Eden: stem cells and their niches."*Science* 287.5457 (2000): 1427-1430.
102. Fuchs, E., Tumbar, T., & Guasch, G. "Socializing with the neighbors: stem cells and their niche." *Cell* 116.6 (2004): 769-778.
103. Campos, L.S. "β1 integrins and neural stem cells: making sense of the extracellular environment." *Bioessays* 27.7 (2005): 698-707.

104. Reichardt, L. F., & Tomaselli, K. J. "Extracellular matrix molecules and their receptors: functions in neural development." *Annual review of neuroscience* 14 (1991): 531.
105. Sanes, J.R. "Extracellular matrix molecules that influence neural development." *Annual review of neuroscience* 12.1 (1989): 491-516.
106. Sobeih, M. M., & Corfas, G. "Extracellular factors that regulate neuronal migration in the central nervous system." *International journal of developmental neuroscience* 20.3 (2002): 349-357.
107. Mahoney, M. J., & Anseth, K. S."Contrasting effects of collagen and bFGF-2 on neural cell function in degradable synthetic PEG hydrogels."*Journal of Biomedical Materials Research Part A* 81.2 (2007): 269-278.
108. Saha, K., Irwin, E. F., Kozhukh, J., Schaffer, D. V., & Healy, K. E. "Biomimetic interfacial interpenetrating polymer networks control neural stem cell behavior." *Journal of Biomedical Materials Research Part A* 81.1 (2007): 240-249.
109. Nakajima, M., Ishimuro, T., Kato, K., Ko, I. K., Hirata, I., Arima, Y., & Iwata, H. "Combinatorial protein display for the cell-based screening of biomaterials that direct neural stem cell differentiation."*Biomaterials* 28.6 (2007): 1048-1060.
110. Stabenfeldt, S. E., Munglani, G., García, A. J., & LaPlaca, M. C. "Biomimetic microenvironment modulates neural stem cell survival, migration, and differentiation." *Tissue Engineering Part A*16.12 (2010): 3747-3758.
111. Johnson, K. R., Leight, J. L., & Weaver, V. M. "Demystifying the effects of a three-dimensional microenvironment in tissue morphogenesis."*Methods in cell biology* 83 (2007): 547-583.
112. Everts, V., van der Zee, E., Creemers, L., & Beertsen, W. "Phagocytosis and intracellular digestion of collagen, its role in turnover and remodelling." *The Histochemical journal* 28.4 (1996): 229-245.
113. Etherington, D.J. "Collagen degradation." *Annals of the Rheumatic Diseases* 36.Suppl 2 (1977): 14-17.
114. Reinhart-King, C. A., Dembo, M., & Hammer, D. A. "Endothelial cell traction forces on RGD-derivatized polyacrylamide substrata." *Langmuir*19.5 (2003): 1573-1579.
115. Reynolds, B. A., Tetzlaff, W., & Weiss, S. "A multipotent EGF-responsive striatal embryonic progenitor cell produces neurons and astrocytes." *The Journal of neuroscience* 12.11 (1992): 4565-4574.
116. Ruoslahti, E. "Brain extracellular matrix." *Glycobiology* 6.5 (1996): 489-492.
117. Ranieri, J. P., Bellamkonda, R., Bekos, E. J., Vargo, T. G., Gardella, J. A., & Aebischer, P. "Neuronal cell attachment to fluorinated ethylene propylene films with covalently immobilized laminin oligopeptides YIGSR and IKVAV. II." *Journal of biomedical materials research* 29.6 (1995): 779-785.
118. Garwood, J., Rigato, F., Heck, N., & Faissner, A. "Tenascin glycoproteins and the complementary ligand DSD-1-PG/phosphacan--structuring the neural extracellular matrix during development and repair." *Restorative neurology and neuroscience* 19.1 (2001): 51-64.

119. Leipzig, N. D., & Shoichet, M. S. "The effect of substrate stiffness on adult neural stem cell behavior." *Biomaterials* 30.36 (2009): 6867-6878.
120. Fan, W., Snyder, M. A., Kumar, S., Lee, P. S., Yoo, W. C., McCormick, A. V., Penn, R.L., Stein, A., & Tsapatsis, M. "Hierarchical nanofabrication of microporous crystals with ordered mesoporosity." *Nature materials* 7.12 (2008): 984-991.
121. Trewyn, B. G., Slowing, I. I., Giri, S., Chen, H. T., & Lin, V. S. Y. "Synthesis and functionalization of a mesoporous silica nanoparticle based on the sol–gel process and applications in controlled release." *Accounts of chemical research* 40.9 (2007): 846-853.
122. Alón, R., Hammer, D. A., & Springer, T. A. "Lifetime of the P-selectin-carbohydrate bond and its response to tensile force in hydrodynamic flow." *Nature* 374.6522 (1995): 539-542.
123. Kong, F., García, A. J., Mould, A. P., Humphries, M. J., & Zhu, C. "Demonstration of catch bonds between an integrin and its ligand." *The Journal of cell biology* 185.7 (2009): 1275-1284.
124. Merkel, R., Nassoy, P., Leung, A., Ritchie, K., & Evans, E. "Energy landscapes of receptor–ligand bonds explored with dynamic force spectroscopy." *Nature* 397.6714 (1999): 50-53.
125. Liu, Z., Tan, J. L., Cohen, D. M., Yang, M. T., Sniadecki, N. J., Ruiz, S. A., Nelson, C.M., & Chen, C. S. "Mechanical tugging force regulates the size of cell–cell junctions." *Proceedings of the National Academy of Sciences* 107.22 (2010): 9944-9949.
126. Smith, J. W., & Cheresh, D. A. "Integrin (alpha v beta 3)-ligand interaction. Identification of a heterodimeric RGD binding site on the vitronectin receptor." *Journal of Biological Chemistry* 265.4 (1990): 2168-2172.
127. Hautanen, A., Gailit, J., Mann, D. M., & Ruoslahti, E. "Effects of modifications of the RGD sequence and its context on recognition by the fibronectin receptor." *Journal of Biological Chemistry* 264.3 (1989): 1437-1442.
128. Nadarajah B, Parnavelas J (2002). "Modes of neuronal migration in the developing cerebral cortex". *Nature Reviews Neuroscience* 3 (6): 423–32
129. Kempermann, G., Jessberger, S., Steiner, B., & Kronenberg, G. "Milestones of neuronal development in the adult hippocampus." *Trends in neurosciences* 27.8 (2004): 447-452.
130. Huang, E. J., & Reichardt, L. F. "Neurotrophins: roles in neuronal development and function." *Annual review of neuroscience* 24 (2001): 677.
131. Pavlou, M. P., Diamandis, E. P., The cancer cell secretome: a good source for discovering biomarkers? *J. Proteomics* 2010, 73,1896–1906.
132. Chiellini, C., Cochet, O., Negroni, L., Samson, M., Poggi, M., Ailhaud, G., Alessi, M.C., Dani, D., & Amri, E. Z.. "Characterization of human mesenchymal stem cell secretome at early steps of adipocyte and osteoblast differentiation." *BMC Molecular Biology* 9.1 (2008): 26.
133. Skalnikova, H., Motlik, J., Gadher, S. J., & Kovarova, H."Mapping of the secretome of primary isolates of mammalian cells, stem cells and derived cell lines." *Proteomics* 11.4 (2011): 691-708.

134. Bendall, S. C., Hughes, C., Campbell, J. L., Stewart, M. H., Pittock, P., Liu, S., Bonneil, E., Thibault, P., Bhatia, M., & Lajoie, G. A.. "An enhanced mass spectrometry approach reveals human embryonic stem cell growth factors in culture." *Molecular & Cellular Proteomics* 8.3 (2009): 421-432.
135. Lodish, H., Berk, A., Zipursky, S. L., Matsudaira, P., et al., *Molecular Cell Biology*, W. H. Freeman, New York 1999.
136. Mortz, E., Krogh, T. N., Vorum, H., & Görg, A. "Improved silver staining protocols for high sensitivity protein identification using matrix-assisted laser desorption/ionization-time of flight analysis." *Proteomics* 1.11 (2001): 1359-1363.

Vita

Emily R. Geishecker was born on July 30, 1987 in Newton, MA to Peg and Steve Geishecker. She grew up in East Walpole, MA and graduated from Walpole High School in 2005. She earned a B.S. in Bioengineering from Lehigh University in May 2009. She joined the Jedlicka Lab in its infancy and continued her undergraduate research in pursuit of her M.S. in Materials Science & Engineering. In addition, she has served as the teaching assistant for Dr. Susan Perry's course, Integrated Biostructural Mechanics Lab, for seven semesters.